Developmental Biology 373 (2013) 39–52

Contents lists available at SciVerse ScienceDirect

Developmental Biology

journal homepage: www.elsevier.com/locate/developmentalbiology

The *Xenopus* doublesex-related gene *Dmrt5* is required for olfactory placode neurogenesis

Damien Parlier [a], Virginie Moers [a], Claude Van Campenhout [a], Julie Preillon [a], Lucas Leclère [b], Amandine Saulnier [a], Maria Sirakov [a], Henriette Busengdal [b], Sadia Kricha [a], Jean-Christophe Marine [c], Fabian Rentzsch [b], Eric J. Bellefroid [a,*]

[a] Laboratoire de Génétique du Développement, Université Libre de Bruxelles, Institut de Biologie et de Médecine Moléculaires (IBMM), rue des Profs. Jeener et Brachet 12, B-6041 Gosselies, Belgium
[b] Sars Centre for Marine Molecular Biology, University of Bergen, N-5008 Bergen, Thormøhlensgt 55, Norway
[c] Laboratory for Molecular Cancer Biology, Department of Molecular and Developmental Genetics, VIB-KULeuven, B-3000 Leuven, Belgium

ARTICLE INFO

Article history:
Received 1 February 2012
Received in revised form
16 September 2012
Accepted 3 October 2012
Available online 9 October 2012

Keywords:
Xenopus
Nematostella
Dmrt
Olfactory placode
OTX2
Notch
Ebf2

ABSTRACT

The *Dmrt* (doublesex and mab-3 related transcription factor) genes encode a large family of evolutionarily conserved transcription factors whose function in sex specific differentiation has been well studied in all animal lineages. In vertebrates, their function is not restricted to the developing gonads. For example, *Xenopus Dmrt4* is essential for neurogenesis in the olfactory system. Here we have isolated and characterized *Xenopus Dmrt5* and found that it is coexpressed with *Dmrt4* in the developing olfactory placodes. As *Dmrt4, Dmrt5* is positively regulated in the ectoderm by neural inducers and negatively by proneural factors. Both *Dmrt5* and *Dmrt4* genes are also activated by the combined action of the transcription factor *Otx2*, broadly transcribed in the head ectoderm and of Notch signaling, activated in the anterior neural ridge. As for *Dmrt4*, knockdown of *Dmrt5* impairs neurogenesis in the embryonic olfactory system and in neuralized animal caps. Conversely, its overexpression promotes neuronal differentiation in animal caps, a property that requires the conserved C-terminal DMA and DMB domains. We also found that the sea anenome *Dmrt4/5* related gene *NvDmrtb* also induces neurogenesis in *Xenopus* animal caps and that conversely, its knockdown in *Nematostella* reduces *elav-1* positive neurons. Together, our data identify *Dmrt5* as a novel important regulator of neurogenesis whose function overlaps with that of *Dmrt4* during *Xenopus* olfactory system development. They also suggest that Dmrt may have had a role in neurogenesis in the last common ancestor of cnidarians and bilaterians.

Introduction

Cranial placodes are transient thickening of the embryonic head ectoderm that give rise to various sensory ganglia and contribute to the pituitary gland and paired sense organs of the head of vertebrate embryos. Despite their different developmental fates, all placodes derive from a common panplacodal primordium around the anterior neural plate, the preplacodal ectoderm. The olfactory placodes develop posterior to the adenohypophyseal placode that appears at the midline of the anterior neural ridge. The inductive events that lead to olfactory placode development remain unclear. It is believed to be a step-wise process that begins with the specification of the preplacodal ectoderm, a step that requires a balance of FGF, BMP and WNT signaling (Litsiou et al., 2005; Ahrens, Schlosser, 2005); Kwon et al., 2010), and continues later with the repression of a lens ground state cell fate and the induction of olfactory placode identity, processes in which FGFs play an important role (Schlosser, 2006, 2010;Streit, 2008;Park and Saint-Jeannet, 2010).

A number of transcription factors have been identified that are expressed at different times and in overlapping patterns during the course of olfactory placode specification and that are required for their development. These factors include Otx2, expressed from the end of gastrulation in all germ layers in a broad anterior domain that includes in the ectoderm the prospective adenohypophyseal, olfactory and lens placodes and the adjacent anterior neural plate (Matsuo et al., 1995; Gammill and Sive, 2001). Proneural genes such as *Ngnr1*, *Ebf2* and *Ath5* are expressed in neurogenic placodes and absent from the regions of the prospective non neurogenic adenohypophysis and lens placodes (Wang et al., 1997, 2004; Nieber et al., 2009; Green and Vetter, 2011). Several Notch ligands are also expressed in the anterior neural

* Corresponding author. Fax: +32 2 650 97 33.
E-mail address: ebellefr@ulb.ac.be (E.J. Bellefroid).

0012-1606/$ - see front matter © 2012 Elsevier Inc. All rights reserved.
http://dx.doi.org/10.1016/j.ydbio.2012.10.003

plate border including the olfactory placodes but little is known today about their function in the developing olfactory epithelium (Chitnis et al., 1995; Peres and Durston, 2006; Schwarting et al., 2007).

The *Dmrt* (*d*oublesex and *m*ab-3 *r*elated *t*ranscription factor) genes encode a large family of evolutionarily conserved transcription factors sharing an unusual zinc finger DNA-binding motif known as the DM domain. *Dmrt* genes are well known for their function in sex determination and sexual dimorphism in invertebrates (Hong et al., 2007; Ross et al., 2005; Kimura et al., 2008). In mammals, most *Dmrt* genes are expressed in the developing gonads. Although not involved in initial sex determination, they are essential for the promotion or maintenance of male specific differentiation. For example, *Dmrt1* has been shown to play a critical role in the gonad in the regulation of hundreds of target genes in both Sertoli cells and germline cells, including genes involved in cell differentiation, cell cycle control and pluripotency (Raymond et al., 2000; Matson et al., 2010, 2011; Murphy et al., 2010). Several of them are expressed and function in nongonadal tissues. For example, the zebrafish gene *terra* and its mouse homolog *Dmrt2* are expressed in the presomitic mesoderm and newly formed somites and play an essential role in somitogenesis (Seo et al., 2006). *Dmrt3* in chicken and mouse embryos is expressed in the forebrain, spinal cord and nasal placode (Meng et al., 1999; Smith et al., 2002). *Dmrt4* in *Xenopus* is expressed in the developing telencephalon and olfactory epithelium and functions as an upstream regulator of proneural genes in the molecular cascade leading to neuronal differentiation in the olfactory system (Huang et al., 2005). *Dmrt5* is expressed in the developing mouse prosencephalon and in the ventral–medial mesencephalic neuroepithelium (Saulnier et al., in press). In neuralized embryonic stem cells, Dmrt5 promotes midbrain dopaminergic identity suggesting that it plays an important role *in vivo* in midbrain ventral progenitor fate (Gennet et al., 2011). In the simple chordate *Ciona, Dmrt1*, the probable ortholog of vertebrate *Dmrt4* and *Dmrt5*, has been shown to be essential for the development of anterior neural plate derivatives (Tresser et al., 2010) suggesting that *Dmrt3–5* genes may play a similar role in vertebrates.

Here we have initiated the characterization of *Dmrt5* in the frog *Xenopus laevis* to approach its function during development. We describe its expression during early embryogenesis, analyse regulatory inputs that control its expression in the ectoderm and the consequences of its knockdown and overexpression on the development of the olfactory epithelium. The data reveal that *Dmrt5* is an important upstream regulator of neurogenesis with redundant roles with *Dmrt4* during olfactory system development. Together with functional and expression data on the sea anenome *Dmrt4/5* related gene *NvDmrtb*, these results suggest that Dmrt may have had a function in neurogenesis in the ancestor of cnidarians and bilaterians.

Material and methods

Isolation of Dmrt5 cDNA and plasmid constructions

The full length *Dmrt5* cDNA clone was isolated by screening a *X. laevis* tadpole head cDNA Library constructed in ZAP II (Hemmati-Brivanlou et al., 1991) using as a probe a PCR generated 580 bp fragment corresponding to the 5′ end of EST CF290698. DNA sequence alignements and phylogenetic trees were obtained using the Clustal method and the MegAlign (DNAStar, Inc) sofware program. Gene synteny analysis was performed using Metazome (http://www.metazome.net). The ORF of *Dmrt5* (accession number DQ329358), *mDmrt2*, *mDmrt3*, *mDmrt5* and *NvDmrtb* were subcloned by PCR into the pCS2+ Myc plasmid. The *Xenopus Dmrt5ΔC* (aa 1–146), *Dmrt5ΔDM* (aa 139–437), *Dmrt5ΔDMAB* (aa 1–258), *Dmrt5ΔDMB* (aa 1–337) and *Dmrt5ΔDMA* (aa 1–258 and 293–437) mutants were generated by PCR and subcloned into the pCS2+ MycNLS vector. All constructs were verified by sequencing. The corresponding proteins were monitored by overexpression in animal caps and western blot analysis using an anti-Myc (clone 9E10, Sigma) primary antibody and a goat anti-mouse IgG secondary antibody conjugated with horseradish peroxydase, followed by detection by chemiluminescence (ECL, Amersham).

Cell culture, transfection and immunolocalization

Cos-7 cells were grown in Dubelcco's modified Eagle's Medium (Gibco-BRL) containing 10% fetal bovine serum (Gibco-BRL), penicillin (50 U/ml), streptomycin (50 mg/ml) and L-glutamine (2 mM) on coverslips and transfected using FUGENE-6 reagent (Roche) according to the manufacturer's instructions. 2 μg of DNA were transfected in 2×10^5 cells with 6 μl FUGENE-6. Cells were fixed 24 h or 48 h after transfection in MEMFA for 15 min, washed two times in PBS and permeabilized in PBS, Triton X-100 0.5% for 10 min at 4 °C. After two washes in PBS, cells were incubated in PBS plus 2% goat serum for 30 min. at RT. The coverslips were incubated with the primary antibody diluted in the former solution for 1 h at RT (anti-Myc,1/500, Sigma) The samples were then washed three times with PBS plus 2% goat serum, and incubated for 1 h with the secondary antibody (Alexa Fluo 488 goat anti-Mouse IgG, Invitrogen). The samples were then washed three times in PBS and incubated 2–3 min in PBS plus Hoechst 0,0005% before mounting.

Emsa

Double strand probes identical to the A, E and F probes (Yi and Zarkower, 1999) were radiolabeled with [$\alpha-{}^{32}$P]dATP by filling in with Klenow fragment. Myc tagged Dmrt5 cloned into the CS2+ vector was synthesized by coupled *in vivo* translation/transcription using Sp6 polymerase and a TNT kit (Promega). EMSA was performed with proteins incubated with 0.5×10^5 cpm of probe (corresponding to about 0,1 ng DNA) in 20 μl of binding buffer as described (Pichon et al., 2004). For supershifts, 1 μl of Myc antibody (Sigma) was added to the binding buffer. Samples were loaded on 4% acrylamide gels and run in 0.5X TBE. Dried gels were exposed to X-ray films overnight at −80 °C in the presence of an intensifying screen.

Xenopus embryo culture, micro-injections and animal cap dissections

Xenopus embryos were obtained from adult frogs by hormone induced egg-laying and *in vitro* fertilization using standard methods (Sive et al., 2000) and staged according to Nieuwkoop and Faber (1967). Synthetic mRNAs were made using Sp6 mMESSAGE mMACHINE. (Ambion). *MT-Dmrt5*, *MT-mDmrt5*, *MT-NLS-Dmrt5ΔC* and *MT-NLS-Dmrt5ΔDM* were linearized with NotI and transcribed with Sp6. Templates described previously include: *MT-Ngnr1* (Ma et al., 1996), *Noggin* (Smith and Harland, 1992), *MT-hGR-EBF2 and MT-hGR-EBF3* (Green and Vetter, 2011), *MT-Ath5* (Burns and Vetter, 2002), *MT-Dmrt4* (Huang et al., 2005); *MT-Otx2-hGR* (Gammill and Sive, 2001) and *MT-hGR-Su(H)Ank-MT* (Wettstein et al., 1997). The *Dmrt5* antisense morpholino (5′-ACC ATT CAG CTC CAT TGT ACA GTT G-3′) and control morpholino oligonucleotides were obtained from Genetools. Dmrt4-MO was previously described (Huang et al., 2005). For *in situ* analysis, embryos were injected in one cell of two to four-cell stage embryos, and fixed at neurula, tailbud or early tadpole stage. In all experiments, embryos were coinjected with *β-gal* mRNA (100 pg/blastomere) to reveal the manipulated side. For animal cap assays, synthesized mRNA was microinjected into the animal region of each blastomere of four-cell

stage embryos. Animal caps were dissected at blastula stage (st.9) and cultured until neurula stage (st.15) for RT-qPCR. Induction of GR constructs was performed by addition of dexamethasone (Dex) around stage 12–13 (10 μM) (Sigma).

RT-PCR and whole-mount in situ hybridization

Total RNA (Quiagen) was extracted using the RNeasy mini kit (Quiagen) or the RNAspin Mini RNA isolation kit (GE Healthcare). All samples were tested for DNA contamination by 30 cycles of PCR amplification using histone H4 primers. cDNA was synthesized with iScript cDNA synthesis kit (Biorad). RT-PCR was done according to Gene Amp PCR kit (Perkin Elmer). Real time RT-PCR was performed using the Step One Plus Real Time PCR system (Applied biosystems) with Q-PCR core kits for SYBR Green I (Eurogentec). Samples were normalized with *Xenopus* GAPDH. The following primers were used: *Dmrt4* (forward 5′-GCCCAAACATGAACCCTAGA-3′ and reverse 5′-GCACCCCTGTCCAGTGATAC-3′); *Dmrt5* (forward 5′ CGGAATCACGGGGTAGTGT-3′ and reverse 5′ TAGTCCTTCGGCAGTTCCAT-3′); *XAG* (forward 5′-CTGACTGTCCGATCAGAC-3′ and reverse 5′-GAGTTGCTTCTCTGGCAT-3′); *Histone H4* (5′-CGGGATAACATTCAGGGTATCACT-3′ and reverse 5′-ATCCATGGCGGTAACTGTCTTCCT-3′); *Ebf2* (forward 5′-TGAGGTGCAACAGAAAAACG-3′ and reverse 5′-CTTCTCCTCACCGAGGACTG-3′); *Neurogenin* (forward 5′-GGCGCGTTAAAGCTAACAAC-3′ and reverse 5′-GCGCAAGGTCTCTATCTTGG-3′); *Sox2* (forward 5′-TGCGTCCAACAACCAGAATA-3′ and reverse 5′-TTGCTGATCTCCGAGTTGTG-3′); Ath5 (forward 5′-GCTGCTATAGGCACTGCTCATAAGG-3′ and reverse 5′-GGCAGACAGAAGCCAGAAAATGGT-3′); *Myt1* (forward 5′-TTGGGATGGTCCCATAGACT-3′ and reverse 5′-TCTTGCATCTCCTGCATCTC-3′) and *GAPDH* (forward 5′-TAGTTGGCGTGAACCATGAG-3′ and reverse 5′-GCCAAAGTTGTCGTTGATGA-3′). All measurements were done in duplicates or triplicates. Error bars represents standard deviation. The values in the figures are representative cases of at least two independent experiments.

Whole-mount *in situ* hybridization analysis was performed as described using digoxigenin- or fluorescein labeled antisense probes (Sive et al., 2000; Bellefroid et al., 1996) generated as indicated: pCMVSport6 Dmrt5 (EST CF290698, SalI/T7), pCMVSport6 Dmrt4 (EST BQ733893, SalI, T7), pbSK(−) Sox2 (EST AF022928, EcoR1, T7). The antisense *Aml* riboprobe was generated from a cDNA fragment encompassing the entire ORF obtained by RT-PCR and subcloned into pZero-2 (Invitrogen) (EcoRI, T7). The following constructs were previously described: *Dlx6* (Luo et al., 2001), *Nkx2.1* (Small et al., 2000), *BF-1* (Bourguignon et al., 1998), *Slug* (Mayor et al., 1995), *Delta1* (Chitnis et al., 1995), *Otx2* (Pannese et al., 1995), *Hes2* (Sölter et al., 2006), *FoxE1* (El-Hodiri et al., 2005), *FoxE3* (Kenyon et al., 1999), *Ebf2* and *Ebf3* (Green and Vetter, 2011), *Neurogenin* (Ma et al., 1996) and *Ep.Keratin* (Jonas et al., 1985). For sections, embryos after completion of the whole-mount procedure were gelatine-embedded and vibratome-sectioned at 30 μm thickness.

TUNEL assays

Whole-mount TUNEL was performed as previously described (Hensey and Gautier, 1998; Yeo and Gautier, 2004) using to reveal the incorporated digoxygenin-dUTP, an anti-digoxigenin antibody coupled to alkaline phosphatase (Roche, 1/2000).

Nematostella experiments

Dmrt genes were identified by Blast search of the *Nematostella* genome (Putnam et al., 2007, http://genome.jgi.doe.gov/Nemve1/Nemve1.home.html) and completed by 5′ and 3′ RACE using the SMART kit (Clontech). Animals were maintained and induced to spawn as described previously (Fritzenwanker and Technau, 2002; Hand and Uhlinger, 1992). *In situ* hybridizations, and microinjections were carried out as described previously (Rentzsch et al., 2006, 2008), mOrange was detected with an anti-dsRed antibody (Clontech 632496). The morpholino sequences are: *NvDmrtb*-5UTR MO: TAACTCACACTACTATGAGGCCGGA, control MO1: CCATTTGAAGTTAAACGATAGATC, control MO2: CCCCATGAACTCTTCCACTAGCCAT. Each morpholino was injected at 0.25 and 0.5 nmol/ml.

Results

Identification of Xenopus laevis Dmrt5

In a microarray screen comparing the transcriptome of wild-type and *Mdm4* mutant brains, which display a high level of apoptosis and a severe deficit in neurogenesis (Martoriati et al., 2005), we identified *Dmrt5* as a gene coding for a potential novel transcriptional factor involved in anterior neural tissue development. To approach its function during embryogenesis, we decided to identify and characterize the orthologous gene in the amphibian *X. laevis* due to the advantages it offers for studying early vertebrate development. Through a BLAST search of the *X. laevis* EST databases, we identified three overlapping partial cDNA clones (accession numbers BJ081978, CF290698 and BG730357) encoding a protein with 48.2% identity over the common region to mouse *Dmrt5* (data not shown). By screening with a 580 bp fragment corresponding to the 5′ end of cDNA CF290698 a tadpole head cDNA library (a gift from A. Hemmati-Brivanlou), we isolated a 2.5 kb full length cDNA clone (accession number DQ329358). The sequence obtained encodes a predicted protein of 437 amino acids that clusters into the DMRTA subfamily (Dmrt3, Dmrt4 and Dmrt5; Suppl. Fig. S1) and is most closely related to Dmrt5 of all vertebrate species (66% identity with human, rat and mouse, 67% with medaka, 70% with zebrafish and 92% with *Xenopus tropicalis*; Fig. 1A). The predicted *X. laevis* Dmrt5 protein contains a N-terminal DM domain that is highly conserved and share 97%–100% identity with those of the other vertebrate Dmrt5 proteins. It also contains two other conserved domains of unknown function called, DMA (aa 259–292) and DMB (338–412) (Fig. 2) present in the C-terminal part of Dmrt5 proteins in vertebrates. The DMA domain is also found in vertebrate Dmrt3 and Dmrt4, suggesting a preferential evolutionary relationship between Dmrt3, Dmrt4 and Dmrt5 (Guo et al., 2004). The orthologous relationship between the *X. tropicalis Dmrt5* gene and the other vertebrate *Dmrt5* genes is also supported by synteny analyses, which show the conservation of genetic linkages between *Dmrt5* and nearby *Faf1* and *Elav* genes (Suppl. Fig. 1B).

To determine the subcellular localization of *X. laevis* Dmrt5, we constructed a plasmid encoding a 6X Myc-tagged version of the protein (MT-Dmrt5), transfected it in COS cells and found that the protein is exclusively detected in the nucleus (Fig. 1B). To determine whether *X. laevis* Dmrt5 exhibits a similar DNA binding specificity to the other Dmrt proteins, we performed electromobility shift assays (EMSA) using an oligonucleotide that contains Mab3 and Dsx binding sites (Yi and Zarkower, 1999) and the Myc tagged Dmrt5 protein. Fig. 1C shows that Dmrt5 strongly shifts the Mab3/Dsx probe (Fig. 1C, lane 2), and that the Dmrt5-specific band can be supershifted by an anti-Myc antibody (lane 3). Binding of Dmrt5 to the *MAB-3* and *DSX* site is specific as it is competed by cold Mab3/Dbx oligonucleotides (lane 4, 5), but not by an oligonucleotide that is bound by the bHLH factor XHRT1 (Pichon et al., 2004) (lane 6, 7). Moreover, changes in the nucleotides that are absolutely required for binding severely affect the binding by Dmrt5 (lane 8, 9). These findings suggest that *X. laevis* Dmrt5 possesses an *in vitro* binding specificity similar to the other Dmrts and further support its identification as a member of the Dmrt class of transcription factors.

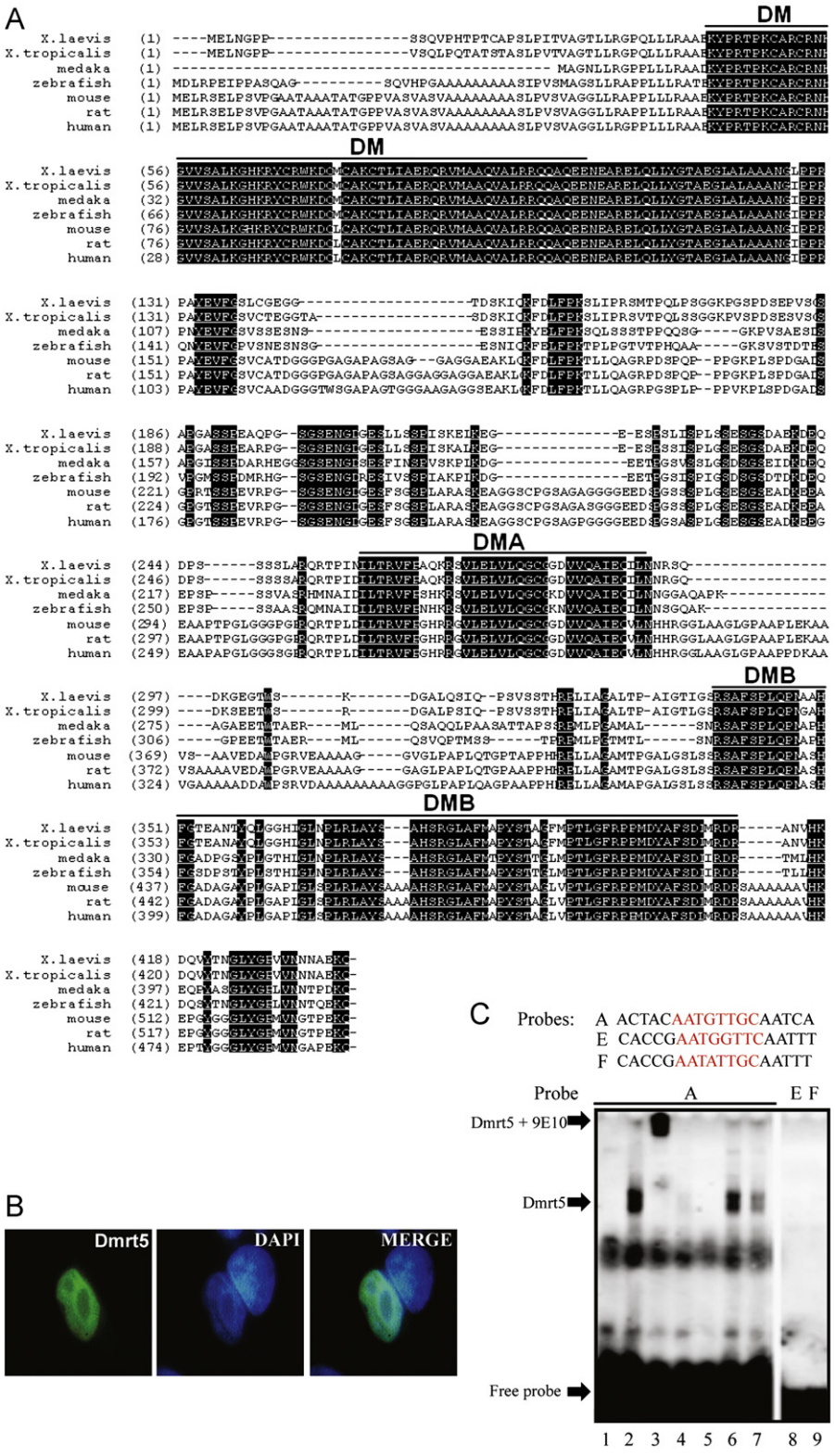

Fig. 1. Sequence, subcellular localization and DNA binding specificity of *Xenopus* Dmrt5. (A) Amino acid sequence alignment of predicted *Xenopus laevis* (DQ 329358), *Xenopus tropicalis* (NP 001096543), medaka (BAD 00703), zebrafish (NP 001007065), mouse (NP 758500), rat (NP 001101421) and human (NP 115486) Dmrt5 proteins. Amino acids conserved in all species are highlighted in black. Dots represent gaps introduced into the sequence in order to obtain optimal sequence homology. The conserved DM, DMA and DMB domains are indicated. (B) pCS2 MT-Dmrt5 transfected COS cells show immunoreactivity restricted to the nucleus (left panel). Nuclei counterstained with DAPI and merge images of the Myc immunostaining and DAPI staining are shown (right panels). (C) EMSA of tagged *Xenopus* Dmrt5 on a labeled Mab3 and Dsx binding site (Yi and Zarkower, 1999). Consensus DNA binding site of Mab3 and Dsx is indicated in red. The position of free probe and shifted complexes containing Dmrt5 are indicated. ^{32}P labeled probe A containing MAB-3 and DSX binding sites was used in lane 1 to 7. Lane 1: reticulocyte lysate only; 2: Myc-tagged Dmrt5; 3: Myc-tagged Dmrt5 plus anti-Myc 9E10 antibody; 4: Myc-tagged Dmrt5 plus 10 × probe A competitor; 5: Myc-tagged Dmrt5 plus 100 × probe A competitor; 6: Myc-tagged xDmrt5 plus 10 × probe HRT1 competitor; 7: Myc-tagged xDmrt5 plus 100 × probe HRT1 competitor. ^{32}P mutated probes E and F were used in lanes 8 and 9, respectively, with Myc-tagged Dmrt5.

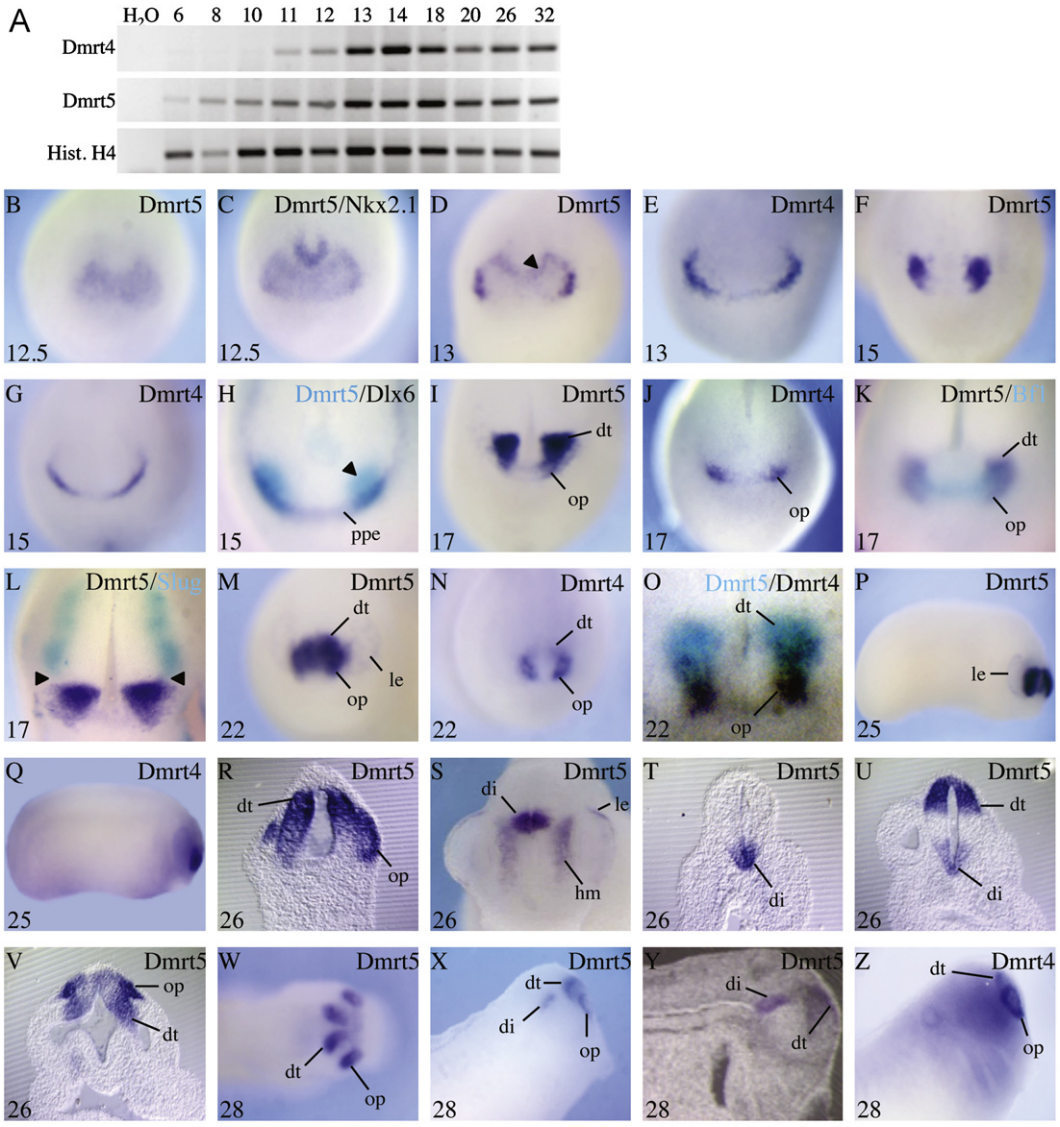

Fig. 2. *Dmrt5* temporal and spatial expression pattern. (A) Temporal expression of *Dmrt5* by RT-PCR. RNA was extracted from embryos at the indicated stages. *Histone H4* was used as a loading control. (B)–(Z) Spatial expression pattern of *Dmrt5* compared to that of *Dmrt4* analysed by whole-mount *in situ* hybridization. Unless indicated, all embryos are shown in anterior views. Nieuwkoop–Faber stages are indicated. (B) Initial expression of *Dmrt5* is observed at stage12.5 in a horse-shoe shaped area in the anterior region of the neurectoderm. (C) Embryo at the stage as in (A) double stained with NBT-BCIP for *Dmrt5* and *Nkx2.1* showing that *Dmrt5* and *Nkx2.1* do not overlap. (D)–(G) At stage 13–15, both *Dmrt5* and *Dmrt4* genes are detected bilateraly at the anterior neural plate border, the *Dmrt5* staining region being broader and extending less medially than the *Dmrt4* stained area. Weak *Dmrt5* expression is also detected at stage 13 in a stripe bordering the posterior side of the initial horse-shoe shaped stained zone (arrowhead). (H) Stage 15 embryo double stained with *Dlx6* (dark blue) and *Dmrt5* (light blue) showing that *Dmrt5* is expressed in a subdomain of the preplacodal ectoderm and that its expression extends to the adjacent neural plate (arrowhead). (I)–(L) Single (I) and (J) and double (K) and (L) *in situ* hybridization showing that at stage 17, *Dmrt5*, but not *Dmrt4*, is coexpressed with *BF-1* in the developping dorsal telencephalon. Note also that *Dmrt5* staining is detected anterior to the domain of expression of the neural crest *Slug* marker. Arrowheads indicate posterior and anterior boundaries of *Dmrt5* and *Slug*, respectively. (M) and (Z) Relationship between the *Dmrt5* and *Dmrt4* genes at stages 22–28, as revealed by single (M)–(Q), (W)–(Z) and double *in situ* hybridization (O). (P), (Q), (X) and (Z) lateral and (W) dorsal views, anterior to the right. A high magnification view of the anterior head fold of a *Dmrt5* and *Dmrt4* double stained embryo is shown in panel O, with *Dmrt5* in light blue and *Dmrt4* in dark blue. (R)–(T) Transverse sections of an embryo through the olfactory epithelium and dorsal telencephalon (R), the anterior (S) or posterior (T) diencephalon. (U) and (V) Horizontal sections though the dorsal telencephalon and diencephalon (U) or through the olfactory placodes and dorsal telencephalon (V). (Y) Sagittal section. Note *Dmrt5* strong expression in the dorsal telencephalon, olfactory placodes and diencephalon and weak expression in the prospective lens ectoderm and in the mesenchyme surrounding the eyes. Abbreviations: dt, dorsal telencephalon; hm, head mesenchyme; le, lens ectoderm; di, diencephalon; op, olfactory placodes; ppe, preplacodal ectoderm.

Dmrt5 expression overlaps with Dmrt4 in the developing olfactory placodes

Semi-quantitative RT-PCR was first used to investigate the temporal expression patterns of *Dmrt5* during early *Xenopus* embryogenesis and to compare it to that of *Dmrt4*. As shown in Fig. 2A, *Dmrt5* was detected maternally and zygotically while *Dmrt4* was only detected zygotically. Zygotic *Dmrt5* transcripts, like those of *Dmrt4*, increase during neurula stages and decrease slightly during the following stages.

In whole-mount *in situ* hybridization, *Dmrt5* transcripts are first detected at early neurula stage (stage 12.5) throughout the anterior portion of the neural plate (Fig. 2B). No expression of *Dmrt4* could be detected at that stage (data not shown). Double *in situ* hybridization with the ventral forebrain marker *Nkx2.1* (Small et al., 2000) indicates that *Dmrt5* expression does not overlap with *Nkx2.1* (Fig. 2C). During later neurula stages, as for *Dmrt4*, strong *Dmrt5* expression was detected in two bilateral patches of cells at the anterior neural plate border. Double *in situ* hybridization using *Dmrt5* and *Dlx6*, highly expressed in the

anterior neural fold in the entire preplacodal ectoderm (Luo et al., 2001; Schlosser, 2006) and single *in situ* of *Dmrt4* and *Dmrt5* shows that *Dmrt5* is expressed in a subdomain of the preplacodal region and that its expression in the panplacodal primordium is more restricted than that of *Dmrt4*, which covers at early stages the adenohypophysis, olfactory and lens placodes (Schlosser, 2006) (Fig. 2D–H). Single and double *in situ* hybridization experiments using *Dmrt5* and *Bf1*, a dorsal telencephalic marker (Bourguignon et al., 1998) show that, in contrast to *Dmrt4*, *Dmrt5* expression extends into the adjacent neural plate (Fig. 2I–K). Double *in situ* with the neural crest *Slug* marker indicates that the posterior domain of *Dmrt5* expression ends anterior to the rostral limit of *Slug*, with a gap detected between the neural crest domain of *Slug* and the *Dmrt5* placodal expression (Fig. 2L). After neural tube closure, *Dmrt5* is strongly expressed in the olfactory placodes and in the telencephalon (Fig. 2M–Z). Around stage 22, as revealed by single and double *in situ*, the expression of *Dmrt5* in the telencephalon is much stronger than that of *Dmrt4* (Fig. 2M–O). Weak *Dmrt5* expression is also detected in the prospective lens ectoderm and in the mesenchyme surrounding the eyes (Fig. 2M, P and S). From stage 25, expression in the olfactory placode and dorsal part of the telencephalon clearly segregates. In contrast to *Dmrt4*, *Dmrt5* is also expressed in the ventral part of the neural tube in a region located rostral to the tip of the notochord that should thus be confined to the diencephalon (Wullimann et al., 2005) (Fig. 2S–U, X, Y). In the telencephalon, *Dmrt5* is restricted to the dorsal pallium compartment and is excluded from the most anterior part of it (Fig. 2R, T–V, Y). Thus, in the frog, *Dmrt5* and *Dmrt4* share overlaping restricted expression patterns during early embryogenesis, with strong early expression in the developing olfactory system.

Dmrt5 and Dmrt4 are differentially induced by BMP antagonists and both genes are downregulated by proneural genes

Dmrt5 expression at the anterior region of the neural plate suggests that it could be regulated by neural inducers. To test this hypothesis, we injected embryos with different doses of the neural inducer Noggin. Animal cap explants were analysed at neurula stage by RT-qPCR for the expression of *Dmrt5* and *Dmrt4*, previously shown to be induced by attenuation of BMPs (Huang et al., 2005). Noggin injected explants showed strong activation of *Dmrt5*. Interestingly, as expected for a neural plate marker, *Dmrt5* was the strongest for the highest dose of *Noggin* mRNA. In contrast, *Dmrt4*, only expressed in the placodes at neurula stage, was induced at the highest level using the lowest dose of *Noggin* mRNA (Fig. 3A). This may be due to the fact that such caps are only partly neuralized and therefore contain non-neural ectoderm from which placodes can arise, which is not the case with caps derived from embryos injected with higher concentration of noggin that are completely converted to neural plate ectoderm. These results indicate that *Dmrt5*, as *Dmrt4*, is positively regulated by attenuation of BMP signaling.

Several HLH transcription factors are sequentially expressed within the olfactory placode during development. In *Xenopus*, the first HLH gene to be expressed in the presumptive olfactory placode is *Ngnr1*, followed by *Ebf2*, *Ebf3* and *Ath5* factors (Burns and Vetter, 2002). Overexpression studies in *Xenopus* have shown that those HLH factors can promote neurogenesis (Ma et al., 1996; Burns and Vetter, 2002; Green and Vetter, 2011). We therefore tested whether *Dmrt5* and *Dmrt4* expression is regulated by those HLH proneural factors. Embryos injected with *MT-Ngnr1, MT-hGR-Ebf2, MT-hGR-Ebf3* or *MT-Ath5* mRNA show a reduction of *Dmrt5* (96%, $n=26$ for *Ngnr1*; 84%, $n=51$ for *Ebf2*; 78%, $n=40$ for *Ebf3* and 72%, $n=18$ for *Ath5*) and of *Dmrt4* (93%, $n=15$ for *Ngnr1*; 54%, $n=28$ for *Ebf2;* 58%, $n=19$ for *Ebf3* and 74%, $n=23$ for *Ath5*) expression on the injected side (Fig. 3B). As previously reported, the pan-neuronal marker *N-tubulin* was in contrast upregulated in those *MT-Ngnr1*, *MT-hGR-Ebf2, MT-hGR-Ebf3* or *MT-Ath5* mRNA injected embryos (data not shown). Thus, as *Dmrt4*, *Dmrt5* is induced by attenuation of BMPs and is downregulated by proneural factors.

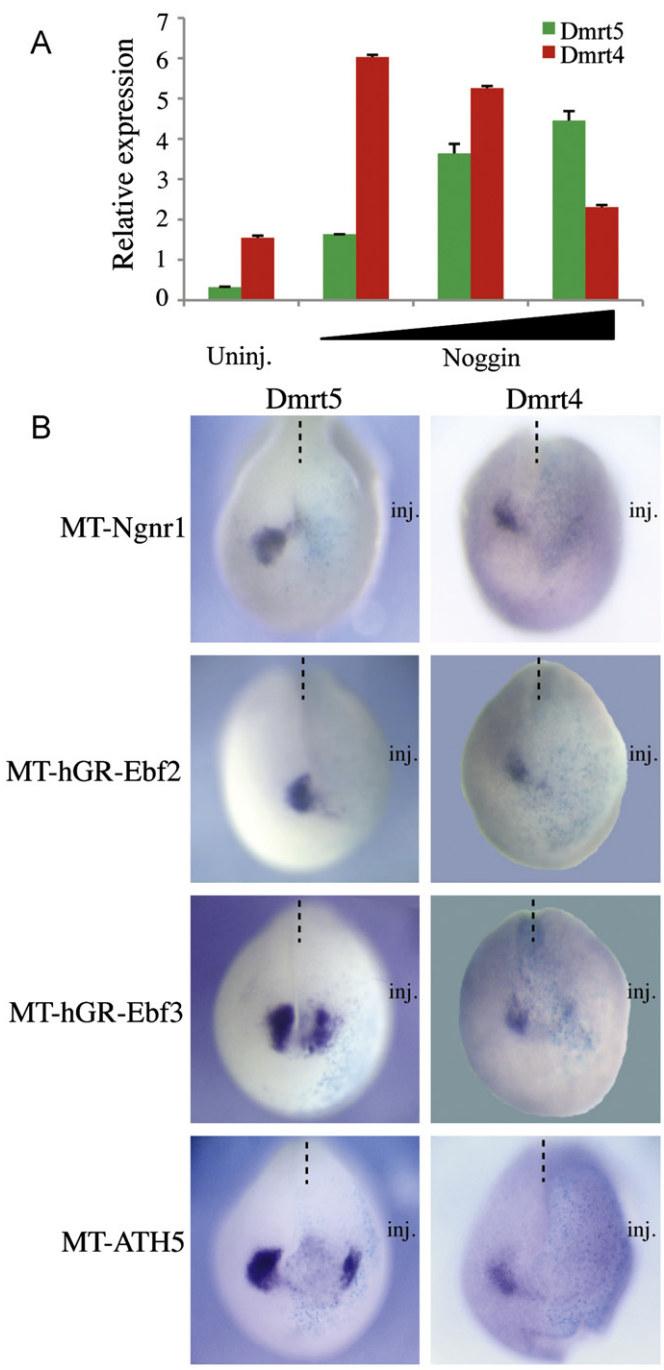

Fig. 3. *Dmrt5* is upregulated by attenuation of BMPs and downregulated by overexpression of the proneural factors *Ngnr1*, *Ebf2, Ebf3 and Ath5*. (A) Real time RT-PCR analysis of animal cap explants isolated from embryos injected with increasing doses of *Noggin* mRNA (40 pg, 100 pg and 400 pg) and collected at stage 17. Note that *Dmrt5* expression is activated by higher doses of *Noggin* mRNA as compared to *Dmrt4*. Each value has been normalized to the level of GAPDH expression. (B) Overexpression of *MT-Ngnr1*, *MT-hGR-Ebf2, MT-hGR-Ebf3* and *MT-Ath5* (400 pg) blocks *Dmrt5* and *Dmrt4* in the embryo. Anterior views of whole-mount *in situ* stained embryos are shown, with dorsal to the top. In all cases, *LacZ* mRNA was used as a lineage tracer to identify the injected side.

Otx2 and Notch activate Dmrt5 and Dmrt4 in the ectoderm

The homeobox gene *Otx2* is a head field selector that is required in the ectoderm for anterior neural determination. It is expressed in the anterior ectoderm including the olfactory placodes and thus coexpressed with *Dmrt5* and *Dmrt4* (Fig. 4A and C). Its overexpression in embryos activates cement gland and anterior neural genes and prevents expression of posterior genes in whole embryos (Gammill and Sive, 2001). To determine whether Otx2 plays a role in *Dmrt5* and *Dmrt4* activation at the anterior neural plate border, embryos were injected with mRNA encoding a glucocorticoid hormone inducible Otx2 construct (*MT-Otx2-hGR*). Dexamethasone (Dex) was added at late gastrula stage (stage 12–13), and expression of *Dmrt5* and *Dmrt4*, was assayed by *in situ* hybridization at stage 25–26. In addition to *Dmrt4* and *Dmrt5*, we also examined expression of the otic placode marker *Hes2* (Sölter et al., 2006), the pituitary marker *FoxE1* (El-Hodiri et al., 2005) and the lens marker *FoxE3* (*lens1*) (Kenyon et al., 1999). We observed that *Otx2*

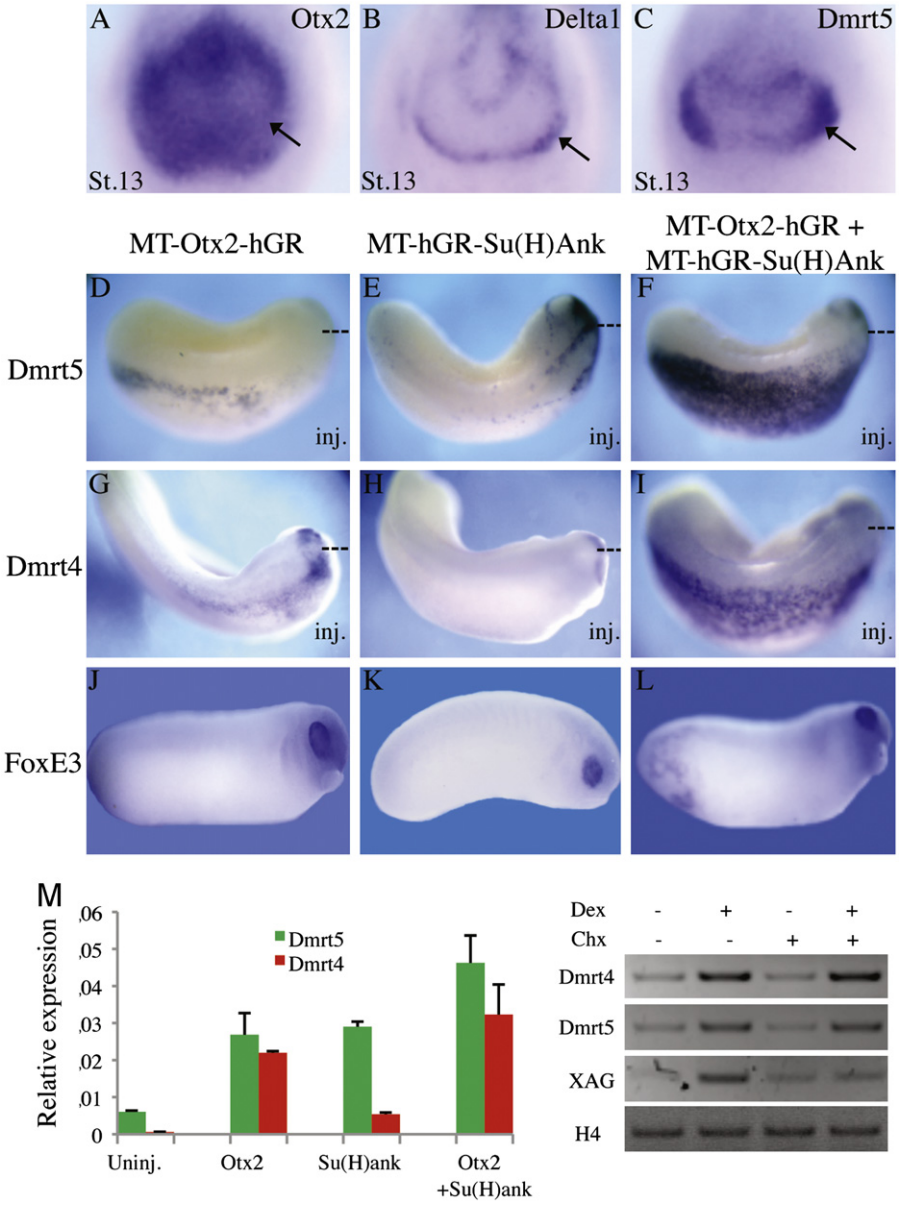

Fig. 4. Combined overexpression of *Otx2* and *Su(H)Ank* efficiently induces ectopic *Dmrt5* and *Dmrt4* expression in the ectoderm. (A)–(C) Anterior views of neurula stage embryos hybridized with *Otx2*, *Delta1* or *Dmrt5*. Arrows indicate the region of the olfactory placodes. (D)-L) Otx2-Notch combined activation in the ectoderm efficiently induces *Dmrt5* and *Dmrt4* expression in the ectoderm. Embryos injected with *MT-Otx2-hGR* and *MT-hGR-Su(H)Ank* (500 pg each) were induced with Dex at stage 12–13, and then subjected to LacZ staining and *in situ* hybridization with the indicated probes. (D)–(I) Dorsal views with anterior to the right. (J)–(L) Lateral views of the injected side. Moderate ectopic *Dmrt4* and *Dmrt5* expression was detected in embryos injected with *Otx2* mRNA alone throughout the ectoderm. While moderate ectopic *Dmrt5* expression mainly restricted to the head ectoderm was also detected in *Su(H)Ank* mRNA injected embryos, no ectopic *Dmrt4* was observed in *Su(H)Ank* mRNA injected embryos. Embryos coexpressing *Otx2* and *Su(H)Ank* show robust ectopic *Dmrt4* and *Dmrt5* staining throughout the ectoderm. *FoxE3* used as control was as previously reported not induced in embryos injected with Otx2 alone or with Su(H)Ank alone injected embryos but was ectopically activated in embryos injected with both constructs. (M) Real time RT-PCR analysis of *Dmrt5* and *Dmrt4* expression in animal caps derived from four-cell stage embryos injected with *MT-Otx2-hGR* or MT-hGR-Su*(H)Ank* mRNA, alone or in combination (500 pg per blastomere). Note that their combination induces stronger expression of *Dmrt5* and *Dmrt4* than that induced by *Otx2* or *Su(H)Ank* alone. Each value has been normalized to the level of *GAPDH* expression. (N) Real time RT-PCR analysis of the expression of *Dmrt5*, *Dmrt4* and *XAG* in animal caps derived from embryos injected with *MT-Otx2-hGR* and MT-hGR-Su*(H)Ank* mRNA, treated or not with dexamethasone (Dex) and cycloheximide (CHX). Note that both *Dmrt5* and *Dmrt4*, but not *XAG*, are activated by *MT-Otx2-hGR* and MT-hGR-Su*(H)Ank* in the presence of CHX.

overexpression causes at both stages moderate ectopic expression of *Dmrt5* and *Dmrt4* in the epidermis (75%, $n=57$ for *Dmrt5* and 41%, $n=37$ for *Dmrt4*) (Fig. 4D and G). No induction of *Hes2* (none, $n=56$) and *FoxE1* (none, $n=27$) was observed. As previously reported (Ogino et al., 2008), *FoxE3* was also unchanged (0%, $n=39$) (Fig. 4J and data not shown). Thus, Otx2 contributes to the activation of *Dmrt5* and *Dmrt4* in the ectoderm.

The Notch ligands *Delta1* and *Delta2* are also expressed during neurulation in the anterior part of the embryo (Fig. 4B). Both genes are detected in a ring surrounding the neural plate, with the highest expression in the region of the olfactory placodes (Chitnis et al., 1995; Bourguignon et al., 1998; Peres and Durston, 2006). To determine whether Notch plays a role in *Dmrt5* and *Dmrt4* activation, embryos were injected with mRNA encoding a glucocorticoid hormone inducible activated form of the Notch effector Su(H), MT-hGR-Su(H)Ank (Wettstein et al., 1997). Dexamethasone was added at stage 12–13 and injected embryos were assayed by *in situ* hybridization at stage 25–26. Embryos injected with *MT-hGR-Su(H)Ank* mRNA exhibited ectopic *Dmrt5* expression in the ectoderm (80% increased, $n=40$). This upregulation of *Dmrt5* in *MT-hGR-Su(H)Ank* mRNA injected embryos was weaker than that observed in *Otx2* overexpressing embryos, and the most robust ectopic expression was often detected in the head ectoderm. No *MT-hGR-Su(H)Ank* mRNA injected embryos with ectopic *Dmrt4* could be observed (none induced, $n=57$)(Fig. 4E and H). *Su(H)Ank* overexpression had also no significant effect on *Hes2* and *FoxE1* (all unaffected, $n=44$ for *Hes2* and 23 for *FoxE1*). As previously reported (Ogino et al., 2008), *FoxE3* was also unchanged (all unaffected, $n=24$) (Fig. 4K and data not shown). These results indicate that Notch plays a role in *Dmrt5* activation in the ectoderm.

Otx2 has been shown to act in concert with Notch signaling to specify the lens-field (Ogino et al., 2008). To determine whether this combination is also involved in controling *Dmrt5* and *Dmrt4* expression, embryos were coinjected with *MT-Otx2-hGR* and *MT-hGR-Su(H)Ank* mRNA. Injected embryos were treated with Dex at stage 12–13 and assayed by *in situ* hybridization at stage 25–26. We observed in those embryos coexpressing *Otx2* and *Su(H)Ank* extensive ectopic *Dmrt5* and *Dmrt4* expression in the entire ectoderm, stronger than that observed in *MT-Otx2-hGR* mRNA alone injected embryos (80%, $n=58$ for *Dmrt5* and 71%, $n=42$ for *Dmrt4*) (Fig. 4F and I). *Hes2* and *FoxE1* were in contrast not activated by the combination of Otx2 and Notch signaling in embryos (none induced, $n=58$ for *Hes2* and 32 for *FoxE1*) (data not shown). As previously reported (Ogino et al., 2008), ectopic *FoxE3* staining could also be detected in response to Otx2 and Notch signaling (28%, $n=40$) (Fig. 4L). Similar results were obtained in animal cap explants cultured until *stage* 25 and analysed by RT-qPCR. In this assay, *Dmrt4* was slightly induced by Su(H)Ank, as *Dmrt5* (Fig. 4M). Upregulation of *Dmrt5* and *Dmrt4* expression was also detected in animal caps derived from embryos overexpressing both *Otx2* and *Su(H)Ank* that were induced with Dex in the presence of a protein synthesis inhibitor, cycloheximide, suggesting a direct effect of MT-Otx2-hGR, MT-hGR-Su(H)Ank or both factors on *Dmrt5* and *Dmrt4* (Fig. 4N). Thus, both Otx2 and Notch play a role in *Dmrt5* and *Dmrt4* activation and their combined activity is sufficient to drive strong ectopic expression in the ectoderm.

Dmrt5, like Dmrt4, is required for neurogenesis

To determine whether *Dmrt5* is required for olfactory placode development, we used a morpholino antisense oligonucleotide designed to interfere with Dmrt5 translation (Dmrt5-MO). The inhibitory efficiency of the Dmrt5-MO was tested *in vivo* by coinjection of the Dmrt5-MO with mRNA encoding a Dmrt5-eGFP fusion construct carrying the targeted sequences. Coinjection of the Dmrt5-MO inhibited the expression of the *Dmrt5*-reporter, but not that of a control *eGFP*-reporter that does not contain the morpholino recognition motif (Fig. 5A). Embryos were injected unilaterally at the two to four cell-stage at the animal pole with 10–20 ng of Dmrt5-MO and analysed at tailbud to tadpole stages by *in situ* hybridization for the expression of the *Ebf2* olfactory placode marker. In Dmrt5-MO injected embryos, expression of *Ebf2* was reduced (70%, reduced, $n=43$) as previously reported in Dmrt4 morphants (Huang et al., 2005) (Fig. 5B and C). Injection of the Dmrt5-MO also inhibited *Ngnr1* and other olfactory markers such as *Aml* and *Ebf3* (80% reduced, $n=25$ for *Ngnr1;* 79% reduced, $n=29$ for *Aml*; 71% reduced, $n=17$ for *Ebf3*) (Fig. 5D–F). By contrast, expression of *FoxE1* expressed in the developing pituitary was unperturbed in Dmrt5 morphants (none affected, $n=23$), as was the expression of *Sox2* (none affected, $n=21$), and *Ep Keratin* (none affected, $n=13$), (Fig. 5G and H and data not shown). Injection at the same dose of a control morpholino had no such effect on the expression of *Ebf2*, *Aml* and *Ebf3* (12% reduced, $n=25$ for *Ebf2*; 8% reduced, $n=12$ for *Aml*; 8% reduced, $n=13$ for *Ebf3*) (Fig. 5I and data not shown). As *Ebf2* is expanded within the developing olfactory placode in *MT-Ath5* mRNA injected embryos (Burns and Vetter, 2002), we also asked whether Dmrt5 is required for the ability of Ath5 to expand *Ebf2*. Fig. 5J and K shows that while *Ebf2* is expanded in *Ath5* overexpressing embryos, it is downregulated in *Ath5* overexpressing Dmrt5 depleted embryos. Attempts to rescue the Dmrt5 MO phenotype in embryos were unsuccessful, most probably because *Dmrt5* overexpression in the conditions used (250–500 pg mRNA per blastomere) affects embryo survival. Indeed, massive dose-dependent apoptosis was detected in *Dmrt5* overexpressing embryos as revealed by TUNEL analysis (Fig. 6A and B). Strong apoptosis was also detected in embryos overexpressing *Dmrt4* (Huang et al., 2005) or mouse *Dmrt5* (37% of embryos, $n=65$ for *Dmrt4* and 77%, $n=30$ for mouse *Dmrt5*) (Fig. 6C and D) and in embryos overexpressing a truncated version of *Dmrt5* lacking the C-terminal region *(MT-NLS-Dmrt5ΔC)* (65%, $n=43$) (Fig. 6E). In contrast, in embryos overexpressing a deletion mutant lacking the N-terminal part, including the DM DNA-binding domain (*MT-NLS-Dmrt5ΔDM*), we did not detect an increase in the frequency of apoptotic cells (96% unaffected, $n=113$) suggesting that it induces apoptosis through its transcriptional regulatory function (Fig. 6F).

To further assess the role of *Dmrt5* in olfactory placode development, we analysed the effects of its depletion on Noggin-mediated neuralization in animal cap explants. Animal caps were collected at stage 14 and analysed by RT-qPCR for the expression of *Ngnr1*, *Ebf2* and *Sox2*. As expected, *Sox2*, *Ngnr1* and *Ebf2* were induced in Noggin injected explants. Coinjection of the Dmrt5-MO decreased the upregulation of *Ngnr1* and *Ebf2* while induction of *Sox2* remained unchanged. To try to rescue the phenotype without inducing a high level of apoptosis, we coinjected the Dmrt5-MO with a low dose of *MT-Dmrt5* mRNA or *MT-mDmrt5* mRNA (50 pg/blastomere). Under these conditions, coinjection of *MT-Dmrt5* mRNA or *MT-mDmrt5* was able to rescue the phenotype (Fig. 5L). To determine whether other neuronal differentiation markers are also reduced after Dmrt5 knockdown in neuralized animal caps, we also analysed at stage 21 the effect of the depletion of Dmrt5 on the general neuronal marker *Myt1* (Bellefroid et al., 1996) and *Ath5* whose expression is restricted at that stage to the olfactory placodes (Kanekar et al., 1997; Burns and Vetter, 2002). Both markers were also reduced in caps derived from Dmrt5-MO injected embryos and the phenotype could be rescued by the overexpression of mDmrt5 (Suppl. Fig. 2). Thus neuronal differentiation is affected in noggin injected caps upon depletion or overexpression of *Dmrt5* and the effect observed could be related to the olfactory placodes.

To further analyse *Dmrt5* function with respect to that of *Dmrt4* in neurogenesis, we first compared the effect of the double

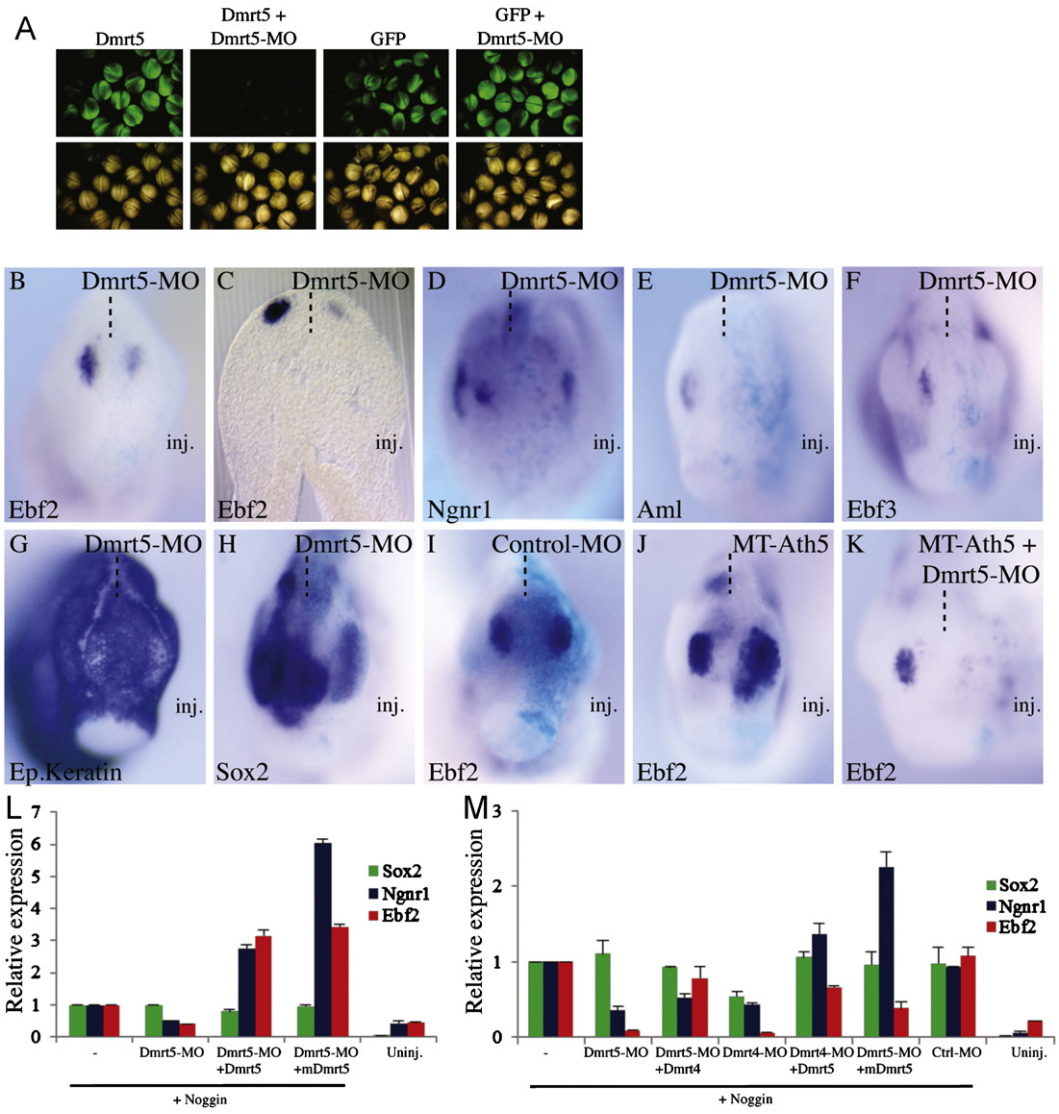

Fig. 5. Knockdown of Dmrt5 reduces *Ngnr1* and *Ebf2* expression. (A) *In vivo* translation of a *Dmrt5-eGFP* reporter construct is specifically inhibited by the Dmrt5-MO. Embryos were injected with 500 pg of *Dmrt5-eGFP* mRNA or, as a control, 500 pg of *eGFP* mRNA, alone or in combination with 20 ng of the Dmrt5-MO, as indicated. (B)–(I) Whole-mount *in situ* hybridization of early tadpole embryos injected with 20 ng of Dmrt5-MO or a control standard MO and analysed with the indicated probes. (B) and (D)–(I) Anterior views with dorsal to the top. (C) Horizontal section through the head, anterior to the top. The injected side marked by Xgal staining in light blue is on the right. Note that Dmrt5 morphants show reduced *Ngnr1*, *Ebf2*, *Aml* and *Ebf3* expression in the olfactory epithelium while *Ep.Keratin* and *Sox2* expression is unaffected. Injection of a control MO has no effect on Ebf2. (J) and (K) Anterior views of early tadpole stage embryos injected with *Ath5* mRNA, with or without 20 ng of DMRT5-MO and hybridised with *Ebf2*. Note that *Ebf2* is expanded in *Ath5* injected embryos and reduced in *Ath5* overexpressing Dmrt5 depleted embryos. (L) and (M) RT-qPCR analysis of *Sox2*, *Ngnr1* and *Ebf2* expression in animal caps derived from embryos injected with *Noggin* (100 pg), *Xenopus MT-Dmrt5* (50 pg), mouse *MT-Dmrt5* (*mMT-Dmrt5*, 50 pg), *Xenopus MT-Dmrt4* (*xDmrt4*, 50 pg), Dmrt4-MO (20 ng) and Dmrt5-MO (20 ng), as indicated. Expression levels were normalized to *GAPDH* and compared to the level observed in *Noggin* injected caps, which was set to 1. Note that Noggin-mediated activation of *Ngnr1* and *Ebf2*, but not that of *Sox2*, is blocked in caps derived from Dmrt5 or Dmrt4 depleted embryos and that their absence can be indifferently rescued by *Dmrt5* or *Dmrt4* overexpression.

Dmrt5–Dmrt4 knockdown to that of the single Dmrt4 or Dmrt5 knockdown using suboptimal doses of the two morpholinos on *Ebf2* in embryos and neuralized animal caps. In both assays, a weak increase in the severity of the phenotype could be observed in double knockdown compared to single knockdown (Suppl. Fig. 3). Next, we tested in animal caps whether Noggin mediated induction of *Ngnr1* and *Ebf2* that is affected by the depletion of Dmrt5 can be rescued by *Dmrt4* overexpression and, conversely, whether the inhibition of these genes in the context of Dmrt4 depleted explants (Huang et al., 2005) can be rescued by *Dmrt5*. Fig. 5M shows that the induction of *Ngnr1* and *Ebf2* in the absence of Dmrt4 can be rescued by overexpression of *Dmrt5* and vice versa. Finally, we asked whether Dmrt4 and Dmrt5 regulate each other. In neuralized animal cap explants, *Dmrt5* was decreased by the Dmrt4-MO. Conversely, *Dmrt4* was reduced by the Dmrt5-MO and this reduction could be rescued by *MT-Dmrt5* overexpression (Suppl. Fig. 4). Together, these results suggest that *Dmrt5* and *Dmrt4* cross regulate each other and that they have overlapping function during olfactory placode neurogenesis. The observation that *Dmrt5* or *Dmrt4* induces massive apoptosis also suggests that a tight control of their expression is required during early development.

Dmrt5 promotes neurogenesis in animal caps

As *Dmrt5* overexpression is able to rescue its depletion in neuralized caps (Fig. 5L), we further studied the role of *Dmrt5* in neurogenesis by overexpressing *Xenopus* or mouse *Dmrt5* in

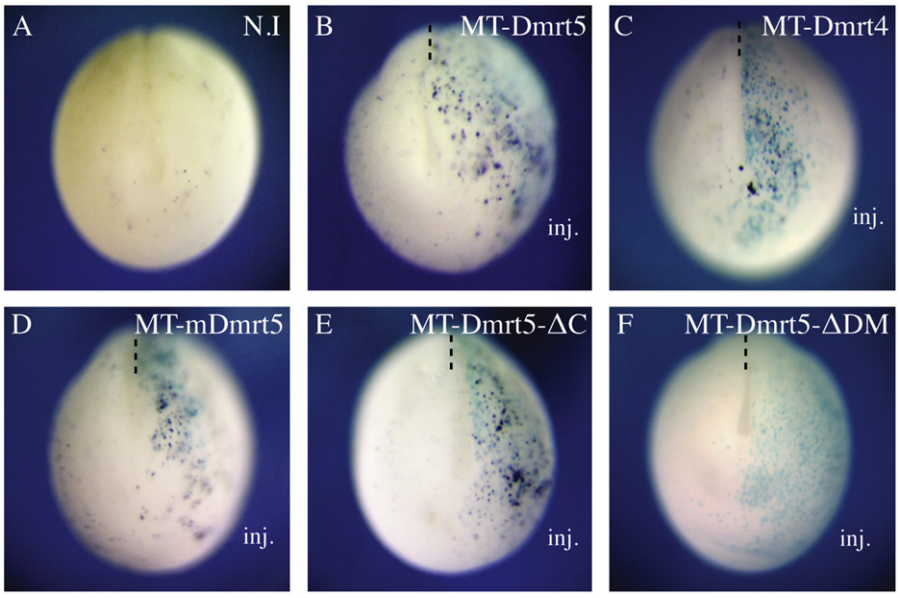

Fig. 6. Increased apoptosis in *Dmrt5* overepressing embryos. (A)–(F) Embryos (stage 15) injected with the indicated Myc-tagged constructs (50 pg) analysed by TUNEL staining. Dorsal views are shown with anterior to the bottom. An increase of staining was detected on the injected side in 93% of embryos, $n=45$ for *MT-Dmrt5*; 51%, $n=74$ for *MT-Dmrt4*; 85%, $n=39$ for *MT-mDmrt5*; 56%, $n=43$ for *MT-Dmrt5ΔC* and 12%, $n=113$ for *MT-Dmrt5ΔDM*.

neuralized animal caps and analysing the caps at early neurula, tailbud, or tadpole stages (stages 14, 22 or 28) by RT-qPCR for *Sox2, Ngnr1* and *Ebf2* expression. *Dmrt5* induces robust expression of *Ngnr1* at stage 14 and to a lesser extend at stage 22. No induction was observed anymore at stage 28. *Ebf2* was also activated at stage 14 and 22 but not at stage 28. In contrast, the level of *Sox2* was not altered by *Dmrt5* overexpression. Western blot analysis revealed decreasing protein levels of MT-Dmrt5 with almost no protein longer detected by stage 28 (Fig. 7A), which explains the absence of ectopic neuronal differentiation at that stage.

As Ath5 regulates neurogenesis in the olfactory placodes (Burns and Vetter, 2002), we tested the ability of *Xenopus* Dmrt5 to influence neuronal differentiation induced by *Xenopus* Ath5 in neurula stage naïve animal caps. Injection of *MT-Dmrt5* mRNA alone slightly induced *Ngnr1* and *Ebf2* and had no effect on *Sox2*. As reported previously, *Ath5* overexpression induces strong *Ebf2* expression (Logan et al., 2005). *Sox2* was also strongly induced by Ath5 and *Ngnr1* was only weakly activated. Interestingly, coexpression of *Dmrt5* together with *Ath5* increases the level of induction of *Ngnr1* and *Ebf2* while the level of *Sox2* induction remains unchanged (Fig. 7B) suggesting that Dmrt5 cooperates with Ath5 to induce olfactory neurogenesis.

To identify the domains of Dmrt5 necessary for its ability to induce neurogenesis, we made a series of constructs encoding myc-tagged Dmrt5 deletion mutants. In addition, we generated constructs encoding mDmrt3, that like Dmrt5 and Dmrt4, contains a DMA domain, and mDmrt2 that lacks this domain. All proteins were detected at the expected size by western blot analysis. Their ability to induce *Ngnr1* and *Ebf2* was tested in neuralized caps at stage 14 by RT-qPCR. *Sox2* which is unaffected by *Dmrt5* overexpression was also examined as a control. No induction of *Ngnr1* and *Ebf2* was observed in animal explants derived from embryos injected with *MT-NLS-Dmrt5ΔC*, *MT-NLS-Dmrt5ΔDM* or *MT-NLS-Dmrt5ΔDMAB* constructs, indicating that both the DM DNA binding domain and the C-terminal region including the conserved DMAB domains is required for Dmrt5 activity. Dmrt5 mutants that only lack either the conserved DMA or DMB domain were also inactive, suggesting that both domains contributes to Dmrt5 activity (Fig. 7C). mDmrt3 was, like mDmrt5 and Dmrt4, able to induce neurogenesis while mDmrt2 failed to do so (Fig. 7D), which further provides evidence for the contribution of the DMA domain to Dmrt's ability to induce neurogenesis.

An ancient role for Dmrt genes in neurogenesis

In order to understand whether a role in neurogenesis is an ancient function of *Dmrt* genes, we turned to the sea anemone *Nematostella vectensis*, a model system from the sister group of bilaterians, the cnidarians. Cnidarian planulae and polyps possess a non-centralized nervous system that consists of sensory cells and ganglion cells, the latter being morphologically equivalent to interneurons (Galliot et al., 2009; Watanabe et al., 2009). In *Nematostella*, neurons are generated in both ecto- and endoderm, commencing in the ectoderm at early gastrula and in the endoderm at planula stage (Nakanishi et al., 2012). The *Nematostella* genome (Putnam et al., 2007) encodes eight *Dmrt* genes, with all of them containing a DMA domain in addition to the DM domain. Phylogenetic analyses based on these two short conserved domains fails to group the *Nematostella* genes unambiguously with the groups of *Dmrt* genes identified in vertebrates (Suppl. Fig. 5A and B and Table S1 related to this figure) and we therefore chose to term them *NvDmrtA-H*. However, we noticed that Bayesian analysis of the DMA domain (or the full length sequences) with a reduced dataset (sequences of vertebrates plus *Nematostella* only) places the *Nematostella NvDmrtb* gene into the Dmrt4/5 group (Suppl. Fig. 5C and data not shown). Expression analysis of this gene by *in situ* hybridization reveals a pattern consistent with a role in neural development. At early gastrula stage, *NvDmrtb* expression can be detected in scattered ectodermal cells in the aboral two thirds of the animal (Fig. 8A). Immediately after the completion of gastrulation the expression remains restricted to the ectoderm but expands into oral and pharyngeal regions (Fig. 8B and C). At midplanula stage expression becomes most prominent in the endoderm, correlating with the onset of endodermal neurogenesis (Fig. 8D, Nakanishi et al., 2012). Higher magnification of some of the *NvDmrtb* positive cells reveals morphologies that resemble the spindle shape of sensory cells (Fig. 8E) and the shape and basal position of ganglion cells (Fig. 8F). To support a possible function of *NvDmrtB* in neural

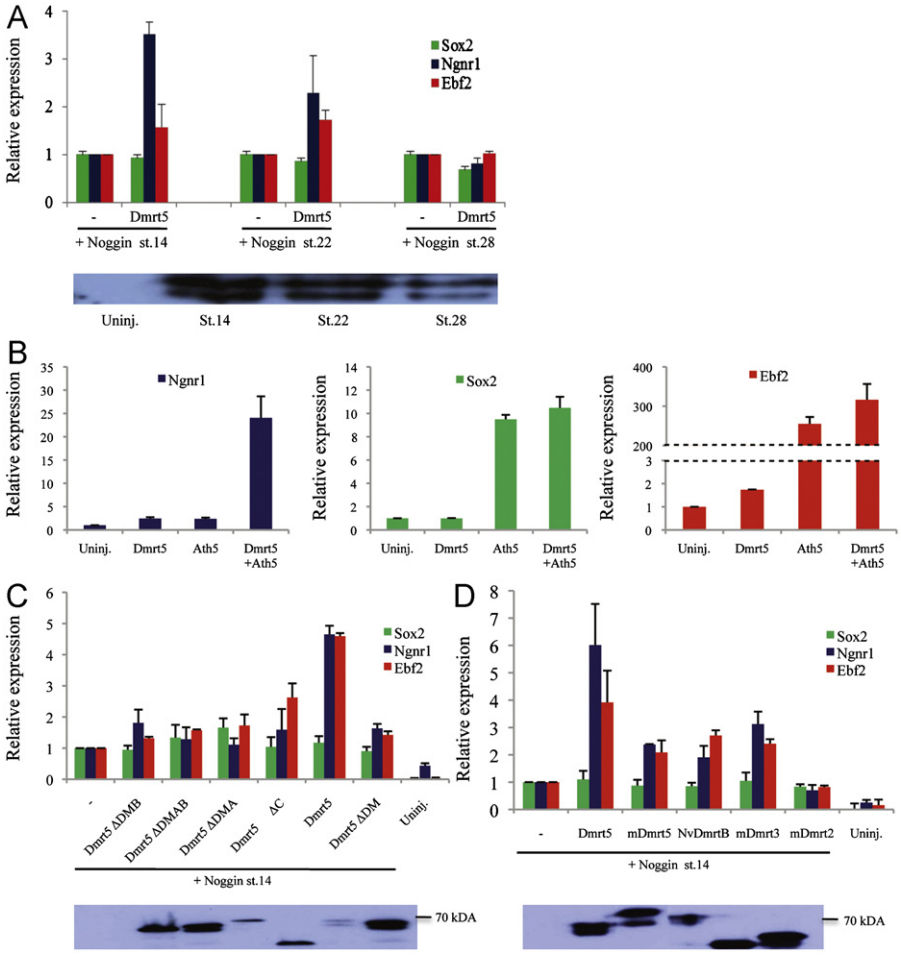

Fig. 7. Regulation of *Sox2, Ngnr1* and *Ebf2* by *Dmrt5*. (A) Animal caps were isolated from embryos injected with *Noggin* (100 pg), *Xenopus MT-Dmrt5* (50 pg) as indicated, cultured until sibling embryos reached stages 14, 22 or 28 and subjected to RT-qPCR analysis. Note that injection of *Xenopus Dmrt5* upregulates *Ngnr1* and *Ebf2* and has no effect on *Sox2* in neuralized caps at stages 14 and 22, but not 28. A control western blot shows the decreasing levels of overexpressed *MT-Dmrt5* in the caps at the different times analysed. (B) Animal caps from embryos injected with *MT-Dmrt5* (50 pg) and *Ath5* (250 pg) as indicated and analysed at stage 14 by RT-qPCR for *Ngnr1, Ebf2* and *Sox2*. Note that Dmrt5 slightly induces *Ngnr1* and *Ebf2* in naïve caps and that it promotes their expression in *MT-Ath5* overexpressing caps while *Sox2* is unaffected. (C) and (D) Animal caps from embryos injected with *Noggin* mRNA (100 pg) alone or coinjected with mRNA encoding the indicated myc-tagged constructs (50 pg each) harvested at stage 14 and analysed by RT-qPCR for *Ngnr1, Ebf2* and *Sox2*. Note that both the DM and the conserved DMA and DMB domains are required for Dmrt5's ability to induce *Ngnr1* and *Ebf2* and that mDmrt3, NvDmrtb but not mDmrt2 induces *Ngnr1* and *Ebf2* expression. In all cases, expression levels were normalized to *GAPDH*. In (A), (C) and (D), expression levels were compared to the level observed in *Noggin* injected caps, which was set to 1. Control western blots showing the overproduced proteins are shown.

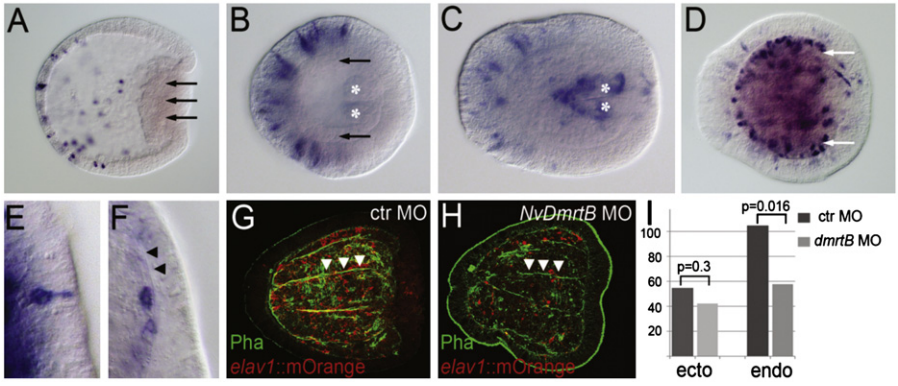

Fig. 8. A *Dmrt* gene is involved in neural development in *Nematostella vectensis*. (A)–(D) In situ hybdridizations with *NvDmrtb* probe at early gastrula (A), late gastrula (B), mid-planula (C) and late planula (D) stage, lateral views, blastopore to the right. Arrows mark the invaginating (A) and epithelial (B) and (D) endoderm, respectively. Asterices indicate the pharynx (B) and (C). (E) and (F) Higher magnification of *NvDmrtb* positive cells with ectodermal sensory cell-like (E) and endodermal ganglion cell-like morphology (F). Black arrowheads label the mesogloea that separates ecto- from endoderm. (G) and (H) Confocal sections of *NvElav1:mOrange* transgenic mid-late planulae injected with 0.5 nmol/ml control MO1 (G) or 0.25 nmol/ml *NvDmrtb* MO (H). Phalloidin-Alexa488 is used to visualize F-actin (green), mOrange is detected by anti-dsRed antibody (red). White arrowheads indicate the longitudinal musculature of one of the eight mesenteries (I) Quantification of morpholino effects. The number of mOrange-positive neurons is reduced in *NvDmrtb* MO injected animals, but only the effect on endodermal neurons is significant ($p=0.016$ for endoderm; $p=0.3$ for ectoderm).

development, we first tested its ability to induce *Ngnr1* and *Ebf2* in neuralized caps at stage 14 by RT-qPCR. As shown above in Fig. 7D, NvDmrtB like Dmrt5, Dmrt4, mDmrt3 and mDmrt5 was able to induce neurogenesis. We next injected a translation blocking morpholino into fertilized eggs from a *NvElav1::mOrange* transgenic *Nematostella* line, in which a large fraction of the ectodermal and endodermal nervous systems are labelled (Nakanishi et al., 2012). Injection of the *NvDmrtB* morpholino, results in a clear reduction of *NvElav1::mOrange* positive neurons in the endoderm compared to injection of two generic control morpholinos, (105.1 (ctr MO1) to 57.8, $n=9$, $p=0.016$, two-tailed Student's *t*-test), whithout affecting overall development or the differentiation of the longitudinal musculature (Fig. 8G–I). The average number of ectodermal *NvElav1::mOrange* positive neurons decreased from 54.9 to 42.2, however, this difference did not reach statistical significance ($n=9$, $p=0.3$). This might reflect the smaller proportion of ectodermal neurons labelled by the transgenic line in comparison to endodermal neurons or a differential requirement for *NvDmrtB* in ecto- vs endodermal neurogenesis.

Discussion

The results presented here strongly suggest that the Dmrt5, which is closely related to Dmrt3–4, plays an important role in neurogenesis during olfactory placode development. We showed that *Dmrt5* is initially coexpressed with *Dmrt4* in the anterior neural ridge in regions that segregate into olfactory placodes and dorsal telencephalon and that, in contrast to *Dmrt4*, it is also later detected in the region of the ventral diencephalon. Homologs of *Dmrt5* have been identified in Platyfish, zebrafish and mouse. In zebrafish, *Dmrt5/Dmrta2* is detected, like in the frog, in the developing olfactory system, dorsal telencephalon and ventral diencephalon (Yoshizawa et al., 2011). In the Platifish and mouse embryos, *Dmrt5* is also expressed in the ventral midbrain (Veith et al., 2006; Gennet et al., 2011; Saulnier et al., in press), which appears not to be the case in the frog. Homologs of *Dmrt4* have been identified in medaka and mouse. In medaka, as in *Xenopus*, *Dmrt4* is expressed in the olfactory placodes and the dorsal telencephalon (Winkler et al., 2004). In the mouse *Dmrta1/Dmrt4* is also expressed in the developing brain (Kim et al., 2003) but its spatial expression has not been investigated. *Dmrt3* has not been identified in *X. laevis*. We found *Dmrt3* however in *Xenopus tropicalis* but could not detect its expression by *in situ* hybridization during early embryogenesis (data not shown). In zebrafish, mouse and chick, *Dmrt3* is also detected in the olfactory placodes and dorsal forebrain. It is also transcribed in spinal cord dorsal interneurons in those species and in the presomitic mesoderm in chicken (Smith et al., 2002; Winkler et al., 2004; Li et al., 2008). Thus, *Dmrt3–5* genes have highly overlapping expression patterns. Their strong expression in the olfactory placodes in all vertebrates examined suggest conserved functions in olfactory system development.

Little is known about the inductive events that initiate olfactory development. In addition to the attenuation of BMPs known to be required for preplacodal ectoderm formation (Brugmann et al., 2004; Glavic et al., 2004; Ahrens and Schlosser, 2005), we found that Otx2 and Notch signaling positively regulate the expression of *Dmrt5* in the ectoderm. Consistent with this idea, *Otx2* is expressed in the mouse as in *Xenopus* in a broad anterior domain of the embryo that includes in the ectoderm of the prospective olfactory placodes (Simeone et al., 1993; Pannese et al., 1995) and blocking Otx2 function in early embryogenesis results in lack of many head structures including the olfactory placodes (Acampora et al., 1995; Matsuo et al., 1995; Gammill and Sive, 2001). Consistent with our data, *Dmrt5* (identified as EST-34) is also induced in an oligonucleotide-based microarray screen performed in animal caps as a target of the endodermal Sox17β transcription factor, a known inducer of *Otx2* (Dickinson et al., 2006). Several members of the Notch pathway are expressed in the mouse olfactory sensory epithelium (Schwarting et al., 2007) and a recent study has shown that Notch activity is required for the maintenance of the proliferative pools of progenitor cells within the olfactory epithelium (Maier et al., 2011). However, the role of Notch signaling in mouse olfactory placode induction remains unknown.

Otx2-Notch interactions have been previously shown to be important in lens determination program (Ogino et al., 2008). Interestingly, we found that the combined overexpression of *Otx2* and activation of Notch induces widespread *Dmrt5* and *Dmrt4* expression in the ectoderm, stronger than that observed in embryos overexpressing *Otx2 or Su(H)Ank* alone, suggesting that this combination may be also used in olfactory placode induction. This hypothesis is further supported by our observation that dominant negative forms of Otx2 (Otx2-En) (Gammill and Sive, 2001) and Su(H) (Su(H)DBM (Wettstein et al., 1997) slightly reduces *Dmrt5* and *Dmrt4* at early neurula stage (data not shown). Further analysis will be needed to determine whether this combination is sufficient to activate later olfactory placode markers. Whether Otx2 and Su(H) input directly on *Dmrt5* cis-regulatory elements remains also to be determined.

Early cell death occurs after neural induction within the neurectoderm and has been shown to be dependent on neurogenesis (Yeo and Gautier, 2004). We found that overexpression of *Dmrt5* and *Dmrt4* induces rapid apoptosis in the embryo. In zebrafish, *Dmrt2/terra* overexpression also induces apoptosis. Whether apoptosis induced by high level of *Dmrt5* expression has no relevance in normal physiological conditions or whether it reflects a role in neurogenesis in the control of cell cyle or proliferation of neural precursors requires further investigation.

The olfactory neuronal transcription factor Olf2/Ebf2 plays an important role in neurogenesis during CNS and olfactory placode development downstream of Ngnr1 (Dubois et al., 1998; Wang et al., 2004). *Dmrt4* is thought to function upstream of these factors in the molecular cascade leading to neuronal differentiation (Huang et al., 2005). In accordance, we found that *Dmrt4* is not activated by *Ngn1*, *Ebf2* and *Ebf3*. The observations that (i) *Ngn1*, *Ebf2* and *Ebf3* do not induce *Dmrt5* (ii) *Ngnr1, Ebf2* and other olfactory markers are blocked in the absence of Dmrt5 (iii) Dmrt5 depletion can be resued by Dmrt4 and vice versa and (iv) Dmrt5 activates *Ngnr1* and *Ebf2* in animal caps and promotes their induction by Ath5 support the hypothesis that *Dmrt5* and *Dmrt4* may function redundantly upstream of *Ngnr1* and *Ebf2* in olfactory placode neurogenesis. In the mouse, *Dmrt4* deficient mice have a histologically normal olfactory epithelium and general olfaction (Balcuniene et al., 2006). *Dmrt4* expression however differs from that in the frog and the *Xenopus Dmrt4* expression pattern more closely resembles that of murine *Dmrt3*, yet. Interestingly, we found that the olfactory epithelium is reduced in *Dmrt5* mutants and is almost completely absent in *Dmrt3:Dmrt5* mutants (Saulnier et al., unpublished data), which further demonstrates the importance of *Dmrt* genes and suggests redundant functions in vertebrate olfactory placode development. To better understand the function of *Dmrt* genes in olfactory system development, it will be important to analyse the phenotype of the *Dmrt5* mutants as well as, due to possible genetic redundancy, that of *Dmrt3:Dmrt5* double mutants.

Mab-3 in *C. elegans* has been suggested to promote the expression of proneural genes in male specific sense organs by preventing the expression of the antineural Hes genes (Ross et al., 2005). Similarly, in zebrafish, it has been recently proposed that Dmrta2/Dmrt5 regulates *neurogenin,* possibly via the repression of *her6* in the telencephalon (Yoshizawa et al., 2011). Whether Dmrt4–5 regulates *Ngnr1* and *Ebf2* in the developing olfactory placodes through a similar mechanism remains to be investigated.

The DMA domain has been reported to be conserved in vertebrate Dmrt3–5 proteins (Guo et al., 2004). Its function is unknown. In our animal assays, we found that Dmrt5 mutants lacking the DMA domain and mDmrt2, which lacks this domain, are inactive, suggesting a role for the DMA domain in the ability of Dmrt proteins to induce neurogenesis. Interestingly, in our search for Dmrt proteins in *N. vectensis*, we found that all eight *Nematostella Dmrt* genes encode DM proteins having a DMA domains and that the DMA domain is also found in other protostomian and deuterostomian *Dmrt* genes (Fig. S4). This suggests that this combination represents the ancestral condition for cnidarians and bilaterians. Similarly, the expression pattern and functional analyses of *NvDmrtb* in *Nematostella* indicate that *Dmrt* genes may have had a role in neural development in the last common ancestor of cnidarians and bilaterians. However, since we could not determine the expression patterns of the other *Nematostella Dmrt* genes, it remains possible that *Dmrt* genes have an additional ancient function in sex determination. These two potential functions may have been present either in one ancestral *Dmrt* gene or in separate paralogs.

Acknowledgements

The authors acknowledge Ali Hemmati-Brivanlou, Robert Grainger, Yasuo Hitoyoshi, Milan Jamrich, Jean-Pierre Saint-Jeannet, Hazel Sive, Monica Vetter and Roberto Vignali for generously providing reagents used in this work and thank Louis Delhaye for excellent technical assistance. This work was supported by grants from the Belgian Fonds de la Recherche Scientifique (FRFC 3.4635.06), the Belgian Queen Elisabeth Medical Foundation, the Van Buuren Foundation, the Fédération Wallonie-Bruxelles (Action de Recherche Concertée), the Interuniversity Attraction Poles Programme, Belgian State, Federal Office for Scientific, Technical and Cultural Affairs (IUAP-P5/35) and the Walloon Region Excellence Programme ("CIBLES"). C.V. is a postdoctoral fellow from the Belgian Fonds de la Recherche Scientifique (FNRS). D. P. and V.M. are doctoral fellows from the Belgian Fonds pour la formation à la Recherche dans l'Industrie et dans l'Agriculture (FRIA). Reserach in F.R.'s lab is funded by the Sars Centre core budget.

Appendix A. Supporting information

Supplementary data associated with this article can be found in the online version at http://dx.doi.org/10.1016/j.ydbio.2012.10.003.

References

Acampora, D., Mazan, S., Lallemand, Y., Avantaggiato, V., Maury, M., Simeone, A., Brulet, P., 1995. Forebrain and midbrain regions are deleted in Otx2$^{-/-}$ mutants due to a défective anterior neurectoderm specification during gastrulation. Development 121, 3279–3290.

Ahrens, K., Schlosser, G., 2005. Tissues and signals involved in the induction of placodal Six1 expression in *Xenopus laevis*. Dev. Biol. 288, 40–59.

Balcuniene, J., Bardwell, V.J., Zarkower, D., 2006. Mice mutant in the DM domain gene Dmrt4 are viable and fertile but have polyovular follicles. Mol. Cell. Biol. 26, 8984–8991.

Bellefroid, E.J., Bourguignon, C., Holleman, T., Ma, Q., Anderson, D.J., Kintner, C., Pieler, T., 1996. X-Myt1, a Xenopus C2HC type zinc finger protein with a regulatory function in neuronal differentiation. Cell 87, 1191–1202.

Bourguignon, C., Li, J., Papalopulu, N., 1998. XBF-1, a winged hélix transcription factor with a dual activity, has a role in positioning neurogenesis in competent ectoderm. Development 125, 4889–4900.

Brugmann, S., Pandur, P., Kenyon, K.L., Pignoni, F., Moody, S.A., 2004. Six1 promotes a placodal fate within the lateral neurogenic ectoderm by functioning as both a transcriptional activator and repressor. Development 131, 5871–5881.

Burns, C.J., Vetter, M.L., 2002. Xath5 regulates neurogenesis in the Xenopus olfactory placode. Dev. Dyn. 225, 536–543.

Chitnis, A., Henrique, D., Lewis, J., Ish-Horowicz, D., Kintner, C., 1995. Primary neurogenesis in Xenopus embryos regulated by a homologue of the *Drosophila* neurogenic gene Delta. Nature 375, 761–766.

Dickinson, K., Leonard, J., Baker, J.C., 2006. Genomic profiling of mixer and Sox17b targets during Xenopus endoderm development. Dev. Dyn. 235, 368–381.

Dubois, L., Bally-Cuif, L., Crozatier, M., Moreau, J., Paquereau, L., Vincent, A., 1998. XCoe2, a transcription factor of the Col/Olf-1/EBF family involved in the specification of primary neurons in Xenopus. Curr. Biol. 8, 199–209.

El-Hodiri, H.M., Seufert, D.W., Nekkalapudi, S., Prescott, N.L., Kelly, L.E., Jamrich, M., 2005. *Xenopus laevis* FoxE1 is primarily expressed in the developing pituitary gland. Int. J. Dev. Biol. 49, 881–884.

Fritzenwanker, J.H., Technau, U., 2002. Induction of gametogenesis in the basal cnidarian *Nematostella vectensis* (Anthozoa). Dev. Genes Evol. 212, 99–103.

Galliot, B., Quiquand, M., Ghila, L., de Rosa, R., Miljkovic-Licina, M., Chera, S., 2009. Origins of neurogenesis, a cnidarian view. Dev. Biol. 332, 2–24.

Gammill, L.S., Sive, H., 2001. Otx2 expression in the ectoderm activates anterior neural determination and is required for xenopus cement gland formation. Dev. Biol. 240, 223–236.

Gennet, N., Gale, E., Nan, X., Farley, E., Takacs, K., Oberwallner, B., Chambers, D., Li, M., 2011. Doublesex and Mab-3-related transcription factor 5 promotes midbrain dopaminergic identity in pluripotent stem cells by enforcing a ventral–medial progenitor fate. Proc. Natl. Acad. Sci. 108, 9131–9136.

Glavic, A., Maris Honoré, S., Gloria, F.C., Bastidas, F., Allende, M.L., Mayor, R., 2004. Role of BMP signaling and the homeoprotein Iroquois in the specification of the cranial placodal field. Dev. Biol. 272, 89–103.

Guo, Y., Li, Q., Gao, S., Zhou, X., He, Y., Shang, X., Cheng, H., Zhou, R., 2004. Molecular cloning, characterization, and expression in brain and gonad of Dmrt5 of zebrafish. Biochem. Biophys. Res. Commun. 324, 569–575.

Green, Y.S., Vetter, M., 2011. EBF factors drive expression of multiple classes of target genes governing neuronal development. Neural Dev. 6, 19.

Hand, C., Uhlinger, K., 1992. The culture, sexual and asexual reproduction, and growth of the sea anemone *Nematostella vectensis*. Biol. Bull. 182, 169–176.

Hemmati-Brivanlou, A., de la Torre, J.R., Holt, C., Harland, R.M., 1991. Cephalic expression and molecular characterization of Xenopus En-2. Development 111, 715–724.

Hensey, C., Gautier, J., 1998. Programmed cell death during Xenopus development: a spatio-temporal analysis. Dev. Biol. 203, 36–48.

Hong, C.-S., Park, B.Y., Saint-Jeannet, J.P., 2007. The function of DMRT genes in vertebrate development: it is not just about sex. Dev. Biol. 310, 1–9.

Huang, X., Hong, C.S., O'Donnell, M., Saint-Jeannet, J.P., 2005. The doublesex-related gene, XDmrt4, is required for neurogenesis in the olfactory system. Proc. Natl. Acad. Sci. 102, 11349–11354.

Jonas, E., Sargent, T.D., Dawid, I.B., 1985. Epidermal keratin gene expressed in embryos of *Xenopus laevis*. Proc. Natl. Acad. Sci. U.S.A 82, 5413–5417.

Kanekar, S., Perron, M., Dorsky, R., Harris, W.A., Jan, L.Y., Jan, Y.N., Vetter, M.L., 1997. Xath5 participates in a network of bHLH genes in the developing Xenopus retina. Neuron 19, 981–994.

Kenyon, K.L., Moody, S.A., Jamrich, M., 1999. A novel fork-head gene mediates early steps during Xenopus lens formation. Development 126, 5107–5116.

Kim, S., Kettlewell, J.R., Anderson, R.C., Bardwell, V.J., Zarkower, D., 2003. Gene Exp. Patterns 3, 77–82.

Kimura, K., Hachiya, T., Koganezawa, M., Tazawa, T., Yamamoto, D., 2008. Fruitless and doublesex coordinate to generate male-specific neurons that can initiate courtship. Neuron 59, 759–769.

Kwon, H.J., Bhat, N., Sweet, E.M., Cornell, R.A., Riley, B.B., 2010. Identification of early requirements for preplacodal ectoderm and sensory organ development. Plos Genet. 6 (9), e1001133, pii.

Li, Q., Zhou, X., Shang, X., Chen, H., Lu, H., Cheng, H., Zhou, R., 2008. Biol. Cell. 100, 453–463.

Litsiou, A., Hanson, S., Streit, A., 2005. A balance of FGF, BMP and WNT signaling positions the future placode territory in the head. Development 132, 4051–4062.

Luo, T., Marsuo-Takasaki, M., Lim, J.H., Sargent, T.D., 2001. Differential regulation of Dlx gene expression by a BMP morphogenetic gradient. Int. J. Dev. Biol. 45, 681–684.

Logan, M.A., Steele, M.R., Van Raay, T.J., Vetter, M.L., 2005. Identification of shared transcriptional targets for the proneural bHLH factors Xath5 and XNeuroD. Dev. Biol. 285, 570–583.

Ma, Q., Kintner, C., Anderson, D.J., 1996. Identification of neurogenin, a vertebrate neuronal differentiation gene. Cell 87, 43–52.

Maier, E., Nord, H., von Hofsten, J., Gunhaga, L., 2011. A balance of BMP and Notch activity regulates neurogenesis and olfactory nerve formation. Plos One 6, e173–179.

Martoriati, A., Doumont, G., Alcalay, M., Bellefroid, E.J., Pelicci, P.G., 2005. dapk1, encoding an activator of a p19ARF-p53-mediated apoptotic checkpoint, is a transcription target of p53. Marine, J.C. 24, 1461–1466Oncogene 24, 1461–1466.

Matson, C.K., Murphy, M.W., Griswold, M.D., Yoshida, S., Bardwell, V.J., Zarkower, D., 2010. The mammalian doublesex homolog DMRT1 is a transcriptional gatekeeper that controls the mitosis versus meiosis decision in male germ cells. Dev. Cell 19, 612–624.

Matson, C.K., Murphy, M.W., Sarver, A.L., Griswold, M.D., Bardwell, V.J., Zarkower, D., 2011. Dmrt1 prevents female reprogramming in the postnatal mammalian testis. Nature 476, 101–104.

Matsuo, I., Kuratani, S., Kimura, C., Takeda, N., Aizawa, S., 1995. Mouse Otx2 functions in the formation and patterning of rostral head. Genes Dev. 9, 2646–2658.
Mayor, R., Morgan, R., Sargent, M.G., 1995. Induction of the prospective neural crest of xenopus. Development 121, 767–777.
Meng, A., Moore, B., Tang, H., Yuan, B., Lin, S., 1999. A *Drosophila* doublesex-related gene, terra, is involved in somitogenesis in vertebrates. Development 126, 1259–1268.
Murphy, M., Sarver, A.L., Rice, D., Hatzi, K., Ye, K., Melnick, A., Heckert, L.L., Zarkower, D., Bardwell, V.J., 2010. Genome-wide analysis of DNA binding and transcriptional regulation by the mammalian Doublesex homolog DMRT1 in the juvenile testis. Proc. Natl. Acad. Sci 107, 13360–13365.
Nakanishi, N., Renfer, E., Technau, U., Rentzsch, F., 2012. Nervous systems of the sea anemone *Nematostella vectensis* are generated by ectoderm and endoderm and shaped by distinct mechanisms. Development 139, 347–357.
Nieber, F., Pieler, T., Henningfeld, K.A., 2009. Comparative expression analysis of the neurogenins in Xenopus tropicalis and *Xenopus laevis*. Dev. Dyn., 451–458.
Ogino, H., Fisher, M., Grainger, R.M., 2008. Convergence of a head-field selector Otx2 and Notch signaling: a mechanism for lens spécification. Development 135, 249–258.
Nieuwkoop, P.D., Faber, J., 1967. Normal table of *Xenopus laevis* (Daudin). North-Holland, Publishing Co, Amsterdam, The Netherlands.
Pannese, M., Polo, C., Andreazzoli, M., Vignali, R., Kablar, B., Barsacchi, G., Boncinelli, E., 1995. The xenopus homologue of Otx2 is a maternal homeobox gene that demarcates and specifies anterior body regions. Development 121, 707–720.
Park, B.Y., Saint Jeannet, J.P., 2010. Induction and Segregation of the Vertebrate Cranial Placodes. Morgan & Claypool Life Sciences, San Rafael,CA.
Peres, J.N., Durston, A.J., 2006. Role of X-Delta2 in the early neural development of *Xenopus laevis*. Dev. Dyn. 235, 802–810.
Pichon, B., Taelman, V., Bellefroid, E.J., Christophe, D., 2004. Transcriptional repression by the bHLH-Orange factor XHRT1 does not involve the C-terminal YRPW motif. Biochem. Biophys. Acta 1680, 46–52.
Putnam, N.H., Srivastava, M., Hellsten, U., Dirks, B., Chapman, J., Salamov, A., Terry, A., Shapiro, H., Lindquist, E., Kapitonov, V.V., Jurka, J., Genikhovich, G., Grigoriev, I.V., Lucas, S.M., Steele, R.E., Finnerty, J.R., Technau, U., Martindale, M.Q., Rokhsar, D.S., 2007. Sea anemone genome reveals ancestral eumetazoan gene repertoire and genomic organization. Science 317, 86–94.
Raymond, C.S., Murphy, M.W., O'Sullivan, M.G., Bardwell, V.J., Zarkower, D., 2000. Dmrt1, a gene related to worm and fly sexual regulators, is required for mammalian testis différentiation. Genes Dev. 14, 2587–2595.
Rentzsch, F., Anton, R., Saina, M., Hammerschmidt, M., Holstein, T.W., Technau, U., 2006. Asymetric expression of the BMP antagonists chordin and gremlin in the sea anemone *Nematostella vectensis*: implications for the evolution of axial patterning. Dev. Biol. 296, 375–387.
Rentzsch, F., Fritzenwanker, J.H., Scholz, C.B., Technau, U., 2008. FGF signalling controls formation of the apical sensory organ in the cnidarian *Nematostella vectensis*. Development 135, 1761–1769.
Ross, J.M., Kalis, A.K., Murphy, M.W., Zarkower, D., 2005. The DM domain protein MAB-3 promotes sex-specific neurogenesis in *C. elegans* by regulating bHLH proteins. Dev. Cell. 8, 881–892.
Saulnier A., Keruzore M., De Clercq S., Bar I., Moers V., Magnani D., Walcher T., Filippis C., Kricha S., Parlier D., Viviani L., Matson C.K., Nakagawa Y., Theil T., Götz M., Mallamaci M., Marine J.-C., Zarkower D., Bellefroid E.J. The doublesex homolog Dmrt5 is required for the development of the caudomedial cerebral cortex in mammals. Cereb. Cortex, http://dx.doi.org/10.1093/cercor/bhs234, in press.
Schlosser, G., 2006. Induction and specification of cranial placodes. Dev. Biol. 294, 303–351.
Schlosser, G., 2010. Making senses development of vertebrate cranial placodes. Int. Rev. Cell Mol. Biol. 283, 129–234.
Schwarting, G.A., Gridley, T., Henion, T.R., 2007. Notch1 expression and ligand interactions in progenitor cells of the mouse olfactory epithelium. J. Mol. Histol. 38, 543–553.
Seo, K.W., Wang, Y., Kobubo, H., Kettlewell, J.R., Zarkower, D.A., Johnson, R.L., 2006. Targeted disruption of the DM domain containing transcription factor Dmrt2 reveals an essential role in somite patterning. Dev. Biol. 290, 200–210.
Simeone, A., Acampora, D., Mallamaci, A., Stornaiuolo, A., Rambaldi, M., Boncinelli, E., 1993. A vertebrate gene related to orthodenticle contains a homeodomain of the bicoid class and demarcates anterior neurectoderm in the gastrulating mouse embryo. EMBO J. 12, 2735–2747.
Sive, H.L., Grainger, R.M., Harland, R.M., 2000. Early Development of *Xenopus laevis*. A laboratory manual. CSHL Press, Cold Spring Harbor, NY.
Small, E.M., Vokes, S.A., Garriok, R.J., Li, D., Krieg, P.A., 2000. Developmental expression of the xenopus Nkx2-1 and Nkx2-4 genes. Mech. Dev. 96, 259–262.
Smith, W.C., Harland, R.M., 1992. Expression cloning of noggin, a new dorsalizing factor localized to the Spemann organizer in Xenopus. Cell 70, 829–840.
Smith, C.A., Hurley, T.M., McClive, P.J., Sinclair, A.H., 2002. Restricted expression of Dmrt3 in chicken and mouse embryos. Gene Exp. Patterns 2, 69–72.
Sölter, M., Locker, M., Boy, S., Taelman, V., Bellefroid, E.J., Perron, M., Pieler, T., 2006. Characterization and function of the bHLH-O protein XHes2: insight into the mechanisms controlling retinal cell fate decision. Development 133, 4097–4108.
Streit, A., 2008. The cranial sensory nervous system: specification of sensory progenitors and placodes. Stembook, Cambridge, MA.
Tresser, J., Chiba, S., Veeman, M., El-Nachef, D., Newman-Smith, E., Horie, T., Tsuda, M., Smith, W.C., 2010. doublesex/mab3 related-1 (Dmrt1) is essential for development of anterior neural plate derivatives in Ciona. Development 137, 2197–2203.
Veith, A.M., Schäfer, M., Klüver, N., Schmidt, C., Schultheis, C., Schartl, M., Volff, J.N., 2006. Tissue-specific expression of *Dmrt* genes in embryos and adults of the platyfish *Xiphophorus maculatus*. Zebrafish 3, 325–337.
Wang, S.S., Tsai, R.Y.L., Reed, R.R., 1997. The characterization of the Olf-1/EBF-Like HLH transcription factor family: implications in olfactory gene regulation and neuronal development. J. Neurosci. 17, 4149–4158.
Wang, S.S., Lewcock, J.W., Feinstein, P., Mombaerts, P., Reed, R.R., 2004. Genetic disruptions of O/E2 and O/E3 genes reveal involvment in olfactory receptor neuron projection. Development 131, 1377–1388.
Watanabe, H., Fujisawa, T., Holstein, T.W., 2009. Cnidarians and the evolutionary origin of the nervous system. Dev. Growth Differ. 51, 167–183.
Wettstein, D.A., Turner, D.L., Kintner, C., 1997. The Xenopus homolog of *Drosophila* Suppressor of hairless mediates Notch signaling during primary neurogenesis. Development 124, 693–702.
Winkler, C., Hornung, U., Kondo, M., Neuner, C., Duschl, J., Shima, A., Schartl, M., 2004. Developmentally regulated and non-sexspecific expression of autosomal *Dmrt* genes in embryos of the medaka fish (oryzias latipes). Mech. Dev. 121, 997–1005.
Wullimann, M.F., Rink, E., Vernier, P., Schlosser, G., 2005. Secondary neurogenesis in the brain of the African Clawed frog, *Xenopus laevis*, as revealed by PCNA, Delta-1, Neurogenin-related-1, and NeuroD expression. J. Comp. Neur. 489, 387–402.
Yeo, W., Gautier, J., 2004. Early neural cell death: dying to become neurons. Dev. Biol. 274, 233–244.
Yi, W., Zarkower, D., 1999. Similarity of DNA binding and transcriptional régulation by Caenorhabditis elegans MAB-3 and *Drosophila* melanogaster DSX suggests conservation of sex determining mechanisms. Development 126, 873–881.
Yoshizawa, A., Nakahara, Y., Izawa, T., Ishitani, T., Tsutsumi, M., Kuroiwa, A., Itoh, M., Kikuchi, Y., 2011. Zebrafish Dmrta2 regulates neurogenesis in the telencephalon. Genes Cells 16, 1097–1109.